Atmos. Chem. Phys. Discuss., doi:10.5194/acp-2016-485, 2016
Manuscript under review for journal Atmos. Chem. Phys.
Published: 14 June 2016
© Author(s) 2016. CC-BY 3.0 License.

Atmospheric Chemistry and Physics Discussions

Differences in BVOC oxidation and SOA formation above and below the forest canopy

Benjamin C. Schulze[1], Henry W. Wallace[1], James H. Flynn[2], Barry L. Lefer[3], Matt H. Erickson[2], B. Thomas Jobson[4], Sebastien Dusanter[5,6,7], Stephen M. Griffith[7,‡], Robert F. Hansen[8,^], Philip S. Stevens[8], Robert J. Griffin[1*]

[1] Department of Civil and Environmental Engineering, Rice University, Houston, TX, 77004

[2] Department of Earth and Atmospheric Sciences, University of Houston, Houston, TX, 77204

[3]Airborne Sciences Program, NASA, Washington, DC, 20546

[4] Department of Civil and Environmental Engineering, Laboratory for Atmospheric Research, Washington State University, Pullman, WA, 99164

[5] Mines Douai, SAGE, F-59508 Douai, France

[6] Université de Lille, 59655 Villeneuve d'Ascq, France

[7] School of Public and Environmental Affairs, Indiana University, Bloomington, IN, USA

[8] Department of Chemistry, Indiana University, Bloomington, IN, USA

[‡]Now at Department of Chemistry, The Hong Kong University of Science and Technology, Kowloon, Hong Kong

[^]Now at School of Chemistry, University of Leeds, Leeds, UK LS2 9JT

[*]Corresponding author: 713-348-2093, rob.griffin@rice.edu

Abstract

Gas-phase biogenic volatile organic compounds (BVOCs) are oxidized in the troposphere to produce secondary pollutants such as ozone (O_3), organic nitrates ($RONO_2$), and secondary organic aerosol (SOA). The nitrate radical (NO_3) is especially reactive towards isoprene and monoterpenes such as α-pinene. A zero-dimensional model has been used to investigate differences in oxidation and SOA production from these two BVOCs, especially with respect to hydroxyl radical (OH) and NO_3, above and below a forest canopy in rural Michigan using local data and data from a monitoring site in Detroit. In all modeled scenarios, NO_3 concentrations are relatively small (0.5-3 pptv); however, daytime concentrations below the canopy are two-to-three times larger than those above. In the rural scenario, NO_3 contributes up to 20% of daytime oxidation of α-pinene below the canopy, and this contribution

Atmos. Chem. Phys. Discuss., doi:10.5194/acp-2016-485, 2016
Manuscript under review for journal Atmos. Chem. Phys.
Published: 14 June 2016
© Author(s) 2016. CC-BY 3.0 License.

Atmospheric Chemistry and Physics Discussions

increases to around 40% in the polluted cases. Oxidation of isoprene is almost entirely dominated by reaction with OH, as expected. The most significant first-generation $RONO_2$ formation mechanism varies significantly between scenarios and by canopy location. Nonetheless, in every scenario, daytime production of first-generation $RONO_2$ through NO_3 + α-pinene is more significant below the canopy than above. While SOA mass loadings are moderate (2 μg m^{-3} or less), total SOA production is consistently enhanced below the canopy, due to the combined effects of elevated isoprene and reduced NO concentrations. Furthermore, below the canopy, the total amount of $RONO_2$ SOA produced through NO_3 oxidation of α-pinene during the daytime (10:00-18:00), while small in absolute terms, is more than twice as large as the amount produced above the canopy during that time period in every scenario. In the rural ambient case, a minimum of 74% of α-pinene $RONO_2$ SOA is formed solely from initial oxidation by NO_3. The relative abundances of HO_2 and NO are shown to substantially impact both total SOA production and $RONO_2$ SOA composition. The results presented emphasize the need for more detailed studies regarding the influence of NO_3 throughout forest canopies in different environments.

Keywords: Nitrate radical, biogenic volatile organic compounds, organic nitrates, secondary organic aerosol

1. Introduction

Globally, organic compounds account for a substantial fraction of total atmospheric aerosol mass (Zhang et al., 2007; Jimenez et al., 2009) and therefore have significant implications for health, visibility, and climate. Rather than being emitted directly, nearly 70% of this material is thought to be secondary organic aerosol (SOA) formed from the oxidation of volatile organic compounds (VOCs) (Hallquist et al., 2009). Many of the relevant VOCs are biogenic in origin, causing naturally emitted compounds to contribute substantially to tropospheric aerosol burdens (Seinfeld and Pankow, 2003). Isoprene (C_5H_8) and monoterpenes ($C_{10}H_{16}$) are important biogenic VOCs (BVOCs) due to their significant rates of emission and reactivity. Studies suggest that together they comprise 55-65% of non-methane VOC emissions globally (Guenther et al., 1995; Hallquist et al., 2009; Guenther et al., 2012) with estimated yearly emissions of 535 Tg and 157 Tg for isoprene and monoterpenes, respectively (Arneth et al., 2011; Guenther et al., 2012). Thus, characterizing the oxidation chemistry and subsequent formation of SOA from BVOCs, especially isoprene and monoterpenes, is critical. Despite continual progress, many questions remain regarding the mechanisms of SOA production, and current large-scale atmospheric models often under-predict organic aerosol (OA) mass loadings (Heald et. al., 2005; Volkamer et al., 2006; Pye and Seinfeld 2010). The focus of this work is the formation of SOA from BVOCs via reaction with various oxidants.

The nitrate radical (NO_3) is known to be a significant nighttime oxidant of a wide range of compounds, including BVOCs (Noxon et al., 1980; Winer et al., 1984; Atkinson and Arey, 2003; Brown and Stutz, 2012). Ambient NO_3 concentrations depend strongly on anthropogenic combustion processes, as the compound is formed from the reaction of ozone (O_3) and nitrogen dioxide (NO_2) and lost, either directly or indirectly, through reaction with nitric oxide (NO) and NO_2. Daytime NO_3 concentrations are generally assumed to be negligible, as rapid photolysis and reaction with NO result in midday lifetimes as low as 5s (Monks, 2005).

Atmos. Chem. Phys. Discuss., doi:10.5194/acp-2016-485, 2016
Manuscript under review for journal Atmos. Chem. Phys.
Published: 14 June 2016
© Author(s) 2016. CC-BY 3.0 License.

Atmospheric Chemistry and Physics Discussions

However, recent work has highlighted the potential for relevant daytime NO_3 concentrations (Geyer et al., 2003a; Brown et al., 2005; Pratt et al., 2012). For example, the shade provided by the forest canopy and corresponding reduction in photolysis rates could result in elevated concentrations near the ground (Brown et al., 2005). Other studies have measured appreciable NO_3 concentrations midday in highly polluted urban environments (Geyer et al., 2003a); however, the effect of the forest canopy in urban areas, where daytime NO_3 loss is largely the result of rapid reaction with NO, has yet to be quantified. As a result, the potential exists for elevated daytime NO_3 oxidation of BVOCs in both below canopy rural environments and polluted urban environments.

The reaction of NO_3 with BVOCs creates organic nitrates ($RONO_2$), which can partition to the particle phase due to the presence of functional groups that lower their volatility. As a result, such products are often particularly important to aerosol production in regions with high biogenic and anthropogenic emissions (Hallquist et al., 1999; Fry et al., 2009, 2011, 2013, 2014; Rollins et al., 2013; Xu et al., 2014, 2015; Lee et al., 2016). In addition, by serving as nitrogen oxide (NO_x = NO + NO_2) reservoirs, $RONO_2$ species influence O_3 production and the oxidative capacity of the atmosphere (Farmer et al., 2001; Wu et al., 2007; Paulot et al., 2012). As the production of $RONO_2$ species has the potential to contribute substantially to tropospheric aerosol mass concentrations, underestimating NO_3 oxidation of BVOCs and subsequent $RONO_2$ production, especially during the day, may partially contribute to the current discrepancy between measured and modeled aerosol mass loadings.

Numerous studies have utilized one-dimensional models to investigate BVOC and radical chemistry within and above forests (Fuentes et al., 2006; Wolfe et al., 2011; Pratt et al., 2012; Rinne et al., 2012; Mogensen et al., 2015); however, to our knowledge only one study has used such a model to investigate SOA production (Ashworth et al., 2015), and the roles of individual oxidants and oxidation products were not explicitly quantified. It has been further hypothesized that differences in NO_3 oxidation chemistry exist between urban and rural forested areas. To investigate these phenomena, we applied a zero-dimensional (0D) model describing BVOC-NO_3-SOA chemistry with a highly detailed chemical mechanism to observations made in both rural and urban environments.

2. Methods

2.1 Description of Model

The 0D model was developed to investigate detailed differences in oxidation chemistry, and as such it involves no atmospheric transport, emissions, or deposition. Rather, for each model scenario, measured diel mixing ratios of gas-phase BVOCs and trace gases (HO_x, O_3, etc.) are used to constrain subsequent modeling of oxidation chemistry and SOA formation. MATLAB computing software (v. R2014a) was used to perform a separate diel analysis of each environment (above and below the canopy) with output every second. The model uses a variable-order ordinary differential equation solver with numerical differentiation formulas to solve the underlying system of differential equations. One day of model spin-up was used for each analysis (Pratt et al., 2012). The oxidation mechanisms of α-pinene and isoprene were obtained directly from the Master Chemical Mechanism (MCM v3.2, via website: http://mcm.leeds.ac.uk/MCM, Jenkin et al., 1997; Saunders et al., 2003), resulting in a system of 2260 chemical reactions with 712 chemical species. These two BVOCs were chosen because of their relatively high emission rates as well as differences in their reactivity and SOA formation potential.

Atmos. Chem. Phys. Discuss., doi:10.5194/acp-2016-485, 2016
Manuscript under review for journal Atmos. Chem. Phys.
Published: 14 June 2016
© Author(s) 2016. CC-BY 3.0 License.

Atmospheric Chemistry and Physics Discussions

The equilibrium gas-particle partitioning model developed by Colville and Griffin (2004) was used to quantify SOA production from individual isoprene and α-pinene oxidation products. To briefly summarize the model, under the assumption that organic aerosol exists primarily in the liquid-phase, an equilibrium partitioning coefficient ($K_{om,i}$, m^3 μg^{-1}) for each oxidation product can be expressed as (Pankow 1994a,b; Odum et al., 1996).

$$K_{om,i} = \frac{A_i}{G_i M_o} = \frac{RT}{MW_{om} 10^6 \gamma_i p^o_{L,i}} \quad (1)$$

where A_i is the amount of species i in the aerosol phase (μg m^{-3}), G_i is the amount of species i in the gas phase (μg m^{-3}), M_o is the total mass of the absorbing phase (μg m^{-3}), R is the ideal gas constant (8.206 x 10^{-5} m^3 atm mol^{-1} K^{-1}), T is the temperature (K), MW_{om} is the average molecular weight of the absorbing phase (g mol^{-1}), γ_i is the activity coefficient of the oxidation product in the aerosol phase (here assumed ideal, γ_i = 1), and $p^o_{L,i}$ is the temperature dependent sub-cooled liquid vapor pressure of the species (atm). The sub-cooled liquid vapor pressure of each oxidation product was determined using the SIMPOL.1 group contribution method (Pankow and Asher, 2008).

Considering this definition in conjunction with the total species concentration (μg m^{-3}), C_i (based on the chemical mechanism described above) and a mass balance for the phase distribution, the following equation can be developed:

$$F(M_o) = \sum_{i=1}^{N} \frac{K_{om,i} C_i}{1 + K_{om,i} M_o} + \frac{POA}{M_o} - 1 \quad (2)$$

where POA represents any initially present OA. Using C_i values determined by the gas-phase mechanism, this equation is solved for M_o at every model time step, from which the value of A_i for each of the N species can be determined. Similarly to Colville and Griffin (2004), the model assumes that, after calculation of A_i values for each species, the total mass of each compound (C_i) is available to react in the gas-phase. Colville and Griffin (2004) have demonstrated that less volatile species, which will have the largest A_i values, are generally less reactive, and therefore this assumption does not greatly affect the model results presented. It should be noted that this partitioning model fails to account for any effects related to the liquid water content (LWC) of SOA or any particle-phase reactions, which, in the case of non-oxidative accretion reactions, have the potential to significantly lower the volatility of the resulting SOA (Kroll and Seinfeld, 2008). Each modeled scenario utilized a POA value of 1 μg m^{-3} in calculation of SOA partitioning, a value slightly higher than previous work (Ashworth et al., 2015) but also slightly lower than the observations made during the same period that are presented in VanReken et al. (2015).

2.2 Input Data

The Community Atmosphere-Biosphere Interactions Experiments (CABINEX) campaign took place in northern Michigan near the University of Michigan Biological Station (UMBS) in August 2009 and utilized the Program on Oxidants: Photochemistry, Emissions, and Transport (PROPHET) tower to perform gas-phase measurements throughout the canopy. A deciduous forest with a canopy height of around 22.5 m surrounds the PROPHET tower and consists of tree species that emit significant quantities of both isoprene (aspen and oak) and monoterpenes (pine and birch). Above canopy measurements were made at a height of 34 m, while those below canopy occurred at a height of 6 m (Fig. S1). More detailed descriptions of both the PROPHET tower and the surrounding environment can be found in the literature (Carroll et al., 2001; Ortega et al., 2007; Griffith et al., 2013).

Atmos. Chem. Phys. Discuss., doi:10.5194/acp-2016-485, 2016
Manuscript under review for journal Atmos. Chem. Phys.
Published: 14 June 2016
© Author(s) 2016. CC-BY 3.0 License.

Atmospheric Chemistry and Physics Discussions

The primary goal of the campaign was to examine the effect of forest succession on atmospheric chemistry. The majority of studies resulting from the CABINEX campaign have focused on improving understanding of the linkage between gas-phase radical and BVOC chemistry through measurements and modeling (Kim et al., 2011; Bryan et al., 2012; Griffith et al., 2013; Hansen et al., 2014), while two have investigated aerosol concentrations at the site (Ashworth et al., 2015; VanReken et al., 2015). Aerosol size and composition vary widely based on ambient wind direction, but show a stronger anthropogenic influence when air masses come from populated areas to the east and south (VanReken et al., 2015), and accurate modeling of diel changes in SOA mass loadings using a 1-D model has proven difficult (Ashworth et al., 2015).

For the scenario termed the ambient CABINEX scenario, the model was constrained by diel median values of hydrogen oxides (HO_x = hydroxyl radical (OH) + hydroperoxy radical (HO_2)), NO_x, O_3, α-pinene (monoterpenes), isoprene, and the photolysis rate of NO_2. The Indiana University Fluorescence by Gas Expansion (IU-FAGE) instrument was used to measure OH and HO_2 (Griffith et al., 2013). Interferences involved in the operation of the IU-FAGE instrument caused slight positive artifacts in the measurement of both OH and HO_2 concentrations. During below canopy measurements, laser photolysis of O_3 within the IU-FAGE sampling cell resulted in a minor artificial increase in OH concentrations, while both above and below the canopy, a fraction of peroxy radicals (RO_2) were converted into HO_2 within the sampling cell, as further explained in Section 2.3.1. The resulting influence of OH on BVOC chemistry in the modeled ambient scenario therefore represents an upper limit, especially below the canopy. Nitrogen oxides were measured using a two-channel chemiluminescense instrument with a blue-light converter for NO_2 measurements (Air Quality Design, Inc.), O_3 was measured using ultraviolet absorption (Thermo Environmental Instruments Inc. 49c), and isoprene and monoterpenes were measured with a proton-transfer reaction mass spectrometer (PTR-MS) (IONICON, Inc.). Gradients above and below the canopy at 6 m and 32 m were measured with the PTR-MS, NO_x, HO_x, and O_3 instruments. As the PTR-MS did not distinguish between monoterpene species, all monoterpenes were assumed to be α-pinene for modeling purposes even though its $RONO_2$ and SOA yields are generally smaller than those of other monoterpene species (Fry et al., 2014; Zhao et al., 2015), potentially resulting in a low bias. This assumption is justified by noting that gas chromatography-mass spectrometry (GC-MS) measurements taken at a height of 6m during CABINEX indicate α-pinene accounted for an average of ~77% of monoterpenes at the site (Wallace, 2013). The photolysis frequency of NO_2 was measured with a Scanning Actinic Flux Spectroradiometer (Flynn et al., 2010). Further information regarding the measurement techniques can be found in Griffith et al. (2013).

Above canopy photolysis frequencies for isoprene and α-pinene oxidation products were obtained directly from the MCM, while photolysis frequencies for other species were taken from the National Center for Atmospheric Research (NCAR) Tropospheric Ultraviolet and Visible (TUV) Model (TUV Model 4.1, via website: http://cprm.acom.ucar.edu/Models/TUV/Interactive_TUV/). In order to correct for non-clear sky conditions, above canopy photolysis frequencies were scaled to represent differences between the measured NO_2 photolysis frequency and that predicted by the TUV model. Below canopy frequencies were then calculated by scaling by the ratio of the below-to-above canopy NO_2 photolysis frequencies measured during CABINEX. This ratio is time-of-day

Atmos. Chem. Phys. Discuss., doi:10.5194/acp-2016-485, 2016
Manuscript under review for journal Atmos. Chem. Phys.
Published: 14 June 2016
© Author(s) 2016. CC-BY 3.0 License.

Atmospheric Chemistry and Physics Discussions

dependent, with a maximum around noon, and varies over the range of 0 to 0.17 (Fig. S2d). Model input data are further described in the Supplemental Information.

At CABINEX, O_3 levels were relatively consistent throughout the diel period, reaching a maximum in the afternoon (Fig. S2). Median mixing ratios were consistently ~5 to 10 ppbv larger above the canopy than below (~30-35 ppbv above, ~20-30 ppbv below). While NO_2 concentrations peaked at night (~1 ppbv), likely due to both O_3 oxidation of local NO and transport from non-local air masses, they were larger below the canopy in the early morning. Concentrations of NO were below the detection limit of the instrument (6.7 pptv) for much of the night and were therefore held at 6.7 pptv for modeling purposes during these periods. Maximum daytime NO mixing ratios reached ~0.2 ppbv in the early morning, largely the result of NO_2 photolysis (Seok et al., 2013). Monoterpene (α-pinene) concentrations were consistent at around 0.2 ppbv, although they exhibit slight diel variability with maxima occurring at night, whereas the isoprene profile displayed strong emission dependence on sunlight and temperature and reached a maximum mixing ratio of ~1.5 ppbv mid-afternoon.

In the second modeled case, from here on labeled the polluted CABINEX scenario, diel O_3 and NO_x profiles were elevated artificially by factors of 2 and 5, respectively, maintaining the ambient NO_2 to NO ratio (NO_2/NO), while all other species and reaction rates were left unchanged. In an ambient environment, changing O_3 and NO_x concentrations alters the modeled diel profile of OH concentrations, potentially affecting the influence of OH on BVOC chemistry (Fig. S3). However, using HO_x concentrations measured during CABINEX as model constraints for each scenario, as was done in this study, rather than allowing the model to predict HO_x concentrations in the second and third scenarios, is the most conservative way to compare the relative role of NO_3 to other oxidants. Specifically, OH concentrations measured during CABINEX are higher than those predicted by the model for the artificially polluted scenario and Detroit scenario both below the canopy for the entire diurnal period and at night in both locations (above and below the canopy) (Fig. S3). As the role of NO_3 relative to other oxidants is maximized under these conditions (below the canopy relative to above and at night relative to during the day), using OH measurements that are higher than model predictions results in the most conservative conclusions about the influence of NO_3 on BVOC chemistry relative to other oxidants. While O_3 and NO_x concentrations similar to those used in this scenario were observed during the PROPHET 1997 campaign (when air masses were transported from more populated areas to the south or southwest) (Carroll et al., 2001; Cooper et al., 2001; Mihele and Haste, 2003), recent campaigns have measured consistently lower concentrations (Griffith et al., 2013; VanReken et al., 2015). As a result, this artificially polluted scenario is meant to represent conditions that might be observed in areas substantially closer to urban metropolitan regions, rather than at the CABINEX site itself.

The third modeled scenario was designed to investigate the impact of a forest canopy within a dense urban region and as such utilized O_3 and NO_2 measurements made by the East 7 Mile Monitoring Station in August 2015 in Detroit (accessed at *www.deqmiair.org*). Detroit air quality monitoring stations do not measure NO concentrations, so the ambient NO_2/NO ratio measured at the Houston Lang C408 and Houston Aldine sites (www.tceq.state.tx.us) in August 2015 were averaged and used to calculate a representative NO diel profile. As isoprene and monoterpene concentrations were not available, they were left unchanged from the CABINEX scenario, as were all photolysis rates. In order to account for "below canopy" O_3 and NO_x levels, measured (and

Atmos. Chem. Phys. Discuss., doi:10.5194/acp-2016-485, 2016
Manuscript under review for journal Atmos. Chem. Phys.
Published: 14 June 2016
© Author(s) 2016. CC-BY 3.0 License.

Atmospheric Chemistry and Physics Discussions

calculated) concentrations in Detroit were scaled by the ratio of below- to above-canopy O_3 and NO_x measurements made during CABINEX. This scenario is ultimately designed to be representative of the boundary of a densely populated region, where an urban emission profile encounters substantial biogenic emissions.

The Detroit data display much more diel O_3 variation, with significant titration around 6 A.M. local time (~15 ppb) and maximum afternoon mixing ratios around 40 ppbv. As both NO_2 and NO display a peak coincident with morning O_3 titration, early morning chemistry appears to be highly related to the urban rush hour. After reaching early morning maximums of 12 and 8 ppbv, respectively, during this period, NO_2 and NO concentrations decrease substantially throughout the morning and afternoon.

2.3 Model Evaluation

2.3.1 HO_x Comparison

Measured OH and HO_2 profiles above the canopy were compared to those predicted by the ambient CABINEX model when leaving HO_x concentrations unconstrained, which gives an indication of the validity of both the modeled oxidation processes and photolysis frequencies, as both have a large effect on HO_x chemistry. The model tends to under predict nighttime OH concentrations, similar to previous model comparisons (Carslaw et al., 2001; Ren et al., 2006; Pugh et al., 2010), while predicting a slightly larger peak concentration (~20% difference) (Fig. S4). On average, nighttime (22:00-6:00 local) modeled OH concentrations are ~$3x10^5$ mol/cm^3 below those observed (~75% difference). As the model only incorporates α-pinene (for all monoterpenes) and isoprene, the absence of OH-producing ozonolysis reactions with other VOCs likely contributes to this nighttime discrepancy. These reactions have been shown to produce up to ~64-72% of nighttime OH in rural environments (Bey et al., 1997; Geyer et al., 2003b). Modeled OH concentrations rise more rapidly after sunrise than those measured. Despite the observed difference in the two profiles, only two measured points (9:00, 17:00) fail to capture modeled concentrations within their 68% confidence intervals. A linear regression of measured versus modeled OH concentrations highlights the ability of the model to capture the diel trend of OH concentrations (r^2 ~0.8) (Fig. S5).

While modeling studies have generally found better performance for HO_2 than for OH, many models involving HO_x cycling in forested environments tend to underestimate HO_2 levels (Lelieveld et al., 2008; Pugh et al., 2010; Stavrakou et al., 2010). Interferences involved in the operation of the IU-FAGE instrument can lead to conversion of isoprene-derived peroxy radicals into HO_2, resulting in a positive artifact (Fuchs et al., 2011). Tests indicate that ~90% of isoprene-based hydroxyalkylperoxy radicals are converted into HO_2 in the sampling cell through reaction with NO and subsequent decomposition (Griffith et al., 2013). As a result, IU-FAGE measurements represent both ambient HO_2 and a fraction of isoprene peroxy radicals chemically converted to HO_2 within the instrument itself. To account for this, simulated isoprene-peroxy radical concentrations were added to simulated HO_2 concentrations when performing a regression analysis.

The agreement between measured and modeled HO_2 concentrations is much more robust than for OH, with the largest difference of 1.43x10^8 mol/cm^3 at 11:00 only 29% smaller than the measured value, likely the result of organic peroxy radical (RO_2) interference (Fig. S4). The HO_2 concentrations are under-predicted midday; however, this result is logical given the interference, as isoprene concentrations are maximized at that time. While the model

Atmos. Chem. Phys. Discuss., doi:10.5194/acp-2016-485, 2016
Manuscript under review for journal Atmos. Chem. Phys.
Published: 14 June 2016
© Author(s) 2016. CC-BY 3.0 License.

Atmospheric Chemistry and Physics Discussions

results successfully represent the overall diel HO_2 profile, the modeled concentration of HO_2 + isoprene RO_2 significantly overestimates measured levels, suggesting either a missing RO_2 loss mechanism, HO_2 loss mechanism, or a combination of both. Good agreement is observed between measured and modeled concentrations with and without the addition of isoprene RO_2 (r^2 = 0.96, slope = 0.69 with RO_2, r^2 = 0.93, slope = 1.04 without). The observation that adding isoprene RO_2 improves the coefficient of determination supports the notion of an isoprene-derived interference (Fig. S5).

2.3.2 NO_3 Steady State and Sensitivity Analysis

Modeled NO_3 concentrations were compared to mathematical predictions assuming steady state conditions. Mathematically, the steady state concentration is estimated by assuming the rate of change of NO_3 (Eq. 3) is zero:

$$\frac{d[NO_3]}{dt} = P - L \quad (3)$$

where P represents the sum of NO_3 production reaction rates and L represents the sum of NO_3 removal reaction rates, each of which are listed below.

Production:

$NO_2 + O_3 \rightarrow NO_3 + O_2$	k_1	(R1)
$N_2O_5 \rightarrow NO_3 + NO_2$	k_2	(R2)

Loss:

$NO_3 + NO \rightarrow 2NO_2$	k_3	(R3)
$NO_3 + h\nu \rightarrow NO + O_2$	J_4	(R4)
$NO_3 + h\nu \rightarrow NO_2 + O(^3P)$	J_5	(R5)
$NO_3 + NO_2 \rightarrow N_2O_5$	k_6	(R6)
$NO_3 + VOC \rightarrow Products$	$\sum_{i=7}^{n} k_i$	(R7)

Reaction rate constants are represented by k_i, while $J_{4,5}$ are the photolysis rate constants for NO_3. Assuming production through dinitrogen pentoxide (N_2O_5) dissociation (R2) is equal to NO_3 loss through reaction with NO_2 (R6), the steady state concentration of NO_3 is

$$[NO_3] = \frac{k_1[NO_2][O_3]}{k_3[NO] + J_4 + J_5 + \sum_{i=7}^{n} k_i[VOC_i]} \quad (4)$$

A regression between modeled and steady state (Eq. 4) NO_3 concentrations yields a coefficient of determination and slope of 0.99, indicating steady state NO_3. As modeled NO_3 concentrations were in fact near steady state, O_3 and NO_2 profiles were systematically altered to test for appropriate changes in the resulting NO_3 concentrations. Scaled changes in NO_2 or O_3 diel profiles should result in proportional changes in NO_3 concentrations. Results using the ambient CABINEX scenario (not shown) agree with this prediction for NO_2 and O_3 perturbations from 50% to 200% of initial levels.

3. Results and Discussion

Atmos. Chem. Phys. Discuss., doi:10.5194/acp-2016-485, 2016
Manuscript under review for journal Atmos. Chem. Phys.
Published: 14 June 2016
© Author(s) 2016. CC-BY 3.0 License.

Atmospheric Chemistry and Physics Discussions

3.1 Nitrate Radical Concentrations

In the ambient scenario, air surrounding the PROPHET tower is free from major NO_x sources, leading to low NO_2 (<1 ppbv) (Fig. S2) and correspondingly low NO_3 concentrations (<1 pptv) (Fig. 1a), despite a relatively high NO_2/NO (median ~12.3). Mixing ratios under 1 pptv agree well with previous results from Mogensen et al. (2015) in a boreal forest setting and Ayres et al. (2015) in rural Alabama. The above-canopy ambient NO_3 profile also agrees well with modeled NO_3 concentrations at the same site for conditions in 2008 (Pratt et al., 2012), which includes more BVOCs but less detail in terms of subsequent oxidation chemistry. The model results presented in Pratt et al. (2012) do not extend below the canopy, preventing a comparison. At night, NO_3 concentrations are enhanced above the canopy compared to below, largely due to larger NO_2 concentrations measured above the canopy during that period. During the day this trend reverses, and mixing ratios are on average twice as large below the canopy compared to above (0.11 pptv below and 0.05 pptv above). As NO_2 concentrations were relatively similar in both locations during the day and O_3 was elevated above the canopy, this observation points to a substantial difference in NO_3 loss rates in the two locations. The effect of NO_3 photolysis specifically is highlighted by the observation of a much stronger diel trend in concentrations above canopy than below.

In the polluted CABINEX scenario (Fig. 1b), NO_3 diel trends are very similar to the ambient case, but the overall levels are enhanced. While NO_3 chemistry is more significant in these more polluted conditions, the relative daytime difference between above and below canopy environments appears to be slightly reduced relative to the ambient CABINEX case. In this polluted environment, midday NO_3 lifetimes with respect to photolysis and reaction with NO are similar (~6s), causing reductions in photolysis rates (i.e., from canopy shade) to have a correspondingly smaller effect on overall NO_3 concentrations.

Modeled NO_3 concentrations in Detroit highlight the difference in gas-phase chemistry between rural and urban environments (Fig. 1c). Specifically, the below-canopy diel NO_3 profile appears to be nearly opposite to the ambient rural scenario, with maximum concentrations during the afternoon and early evening rather than at night. The observation of midday concentrations as large or larger than those at night contrasts previous urban measurements where, despite measuring midday concentrations up to 1 pptv, observed nighttime concentrations reached levels 50 times as large (Geyer et al. 2003a). It should be reemphasized that for this modeling study, above/below canopy ratios measured in a rural environment were used to calculate "below-canopy" concentrations of O_3, NO, and NO_2 in Detroit, as measurements from the Detroit monitor were assumed to be "above-canopy". The amount of error introduced by this assumption is left undefined; however, median maximum O_3 concentrations of only around 40 ppbv ultimately prevent appreciable NO_3 production (<1 pptv), even in this urban setting. As a result, while below-canopy concentrations may be artificially elevated to some extent, the relatively small concentrations in Detroit air results in absolute NO_3 concentrations smaller than those observed in other more polluted cities (Houston, Atlanta, etc.) (Geyer et al 2003a, Matsumoto et al., 2005; Stutz et al., 2010; Brown and Stutz 2012).

Minimum NO_3 concentrations in the Detroit scenario are observed during the early morning rush hour (~6 AM) as vehicular NO_x emissions, virtually absent in the rural scenario, reduce O_3 and NO_3 concentrations while photolytic NO_3 loss rates simultaneously increase. After that period, from 6:00-9:00, the substantial increase in

Atmos. Chem. Phys. Discuss., doi:10.5194/acp-2016-485, 2016
Manuscript under review for journal Atmos. Chem. Phys.
Published: 14 June 2016
© Author(s) 2016. CC-BY 3.0 License.

Atmospheric Chemistry and Physics Discussions

below-canopy NO_3 concentrations relative to above results primarily from an NO_2/NO ratio much larger than that above the canopy (factor of 3.6) combined with reduced photolysis rates. The relative difference between daytime above- and below-canopy NO_3 concentrations is more significant in this scenario than in either CABINEX case (2 to 5 times higher below-canopy). During this period, reaction with NO acts as the major NO_3 loss mechanism (NO_3 lifetime of ~2s with respect to NO reaction), in agreement with previous urban NO_3 studies (Geyer et al., 2003a). These results indicate that even in urban environments, substantially elevated NO_3 concentrations are possible below a forest canopy.

3.2 Daytime Below-Canopy NO_3 Enhancement

A detailed analysis of NO_3 production and loss processes was performed in order to specify the reasons for daytime elevation of NO_3 concentrations under the canopy, with a specific focus on the ambient CABINEX scenario. The three major NO_3 loss mechanisms are oxidation of VOCs (isoprene and α-pinene in this model), reaction with NO, and photolysis.

Photolysis is the major above-canopy NO_3 loss process during the day (lifetime ~5s), while α-pinene oxidation is the most important below-canopy daytime loss (~30s) (Fig. 2). Nighttime NO_3 loss is dominated by α-pinene oxidation both above and below the canopy (~40s). In terms of relative NO_3 production, rates are highest above the canopy in the early morning hours (0:00-6:00), below the canopy midmorning (6:00-12:00), and similar above and below the canopy in the afternoon and evening (Fig. 3). From 6:00-12:00, the modeled enhancement of NO_3 below the canopy is primarily the result of increased production, as loss rates are similar. However, from 12:00-18:00, production rates are similar in both environments, and loss rates from NO and VOCs are higher below-canopy than above. As a result, reduced below-canopy NO_3 photolysis is the primary contributor to the observation of elevated below-canopy NO_3 concentrations in the afternoon. Therefore, in rural environments, canopy shade and the corresponding reduction in photolysis rates appear to directly increase the importance of daytime NO_3 chemistry.

3.3 BVOC Oxidation

Numerous studies have investigated NO_3 oxidation of BVOCs and highlighted that such oxidation is especially important at night (Golz et al., 2001; Brown et al., 2005; Brown et al., 2011; Stutz et al., 2010; Brown and Stutz, 2012). Certain classes of BVOCs also show appreciable daytime oxidation rates by NO_3 (Geyer et al., 2003a; Brown et al., 2005). The prediction of elevated daytime NO_3 concentrations below the forest canopy implies an increased rate of BVOC oxidation in that environment. Oxidation rates (and fractional contributions of the total) by each oxidant are determined by

$$\text{Oxidation Rate (ppbv hr}^{-1}) = k\,[\text{Oxidant}][\text{VOC}] \quad (5)$$

Ambient CABINEX results (Figs. 4 and 5) show that overall rates of α-pinene oxidation above and below the canopy are similar (~0.08 ppbv hr^{-1}), while the fractional plots indicate that in both cases, O_3 is the most consistent oxidant, contributing over 40% of total oxidation. Hydroxyl radical oxidation reaches maximum contributions of 66% above the canopy and 63% below the canopy near midday (Fig. 5). The NO_3 oxidation rates largely reflect the NO_3 concentration profile, as α-pinene concentrations are consistent throughout the 24-hour

Atmos. Chem. Phys. Discuss., doi:10.5194/acp-2016-485, 2016
Manuscript under review for journal Atmos. Chem. Phys.
Published: 14 June 2016
© Author(s) 2016. CC-BY 3.0 License.

Atmospheric Chemistry and Physics Discussions

period, with above canopy rates displaying more diel variation than those below due to the substantial effect of NO_3 photolysis. Oxidation by NO_3 contributes 18% of total oxidation above the canopy on average and 19% below. Perhaps the most substantial difference between the two environments occurs from around 8 AM to 8 PM, as NO_3 contributes on average only 5% of total α-pinene oxidation above the canopy but as much as 14% below.

The α-pinene oxidation profiles for the polluted CABINEX scenario show noticeably enhanced contributions from NO_3, altering the entire diel oxidation pattern. Maximum oxidation rates in this case (~0.2-0.3 ppbv hr^{-1}) occur at night when photochemical activity and the corresponding influence from OH are nearly negligible. For roughly 9 hours (21:00-6:00) the overall NO_3 contribution is greater than 60% of total oxidation. Oxidation by OH never exceeds half of the total in either environment, while O_3 oxidation on a relative scale is similar to the ambient case, despite O_3 concentrations having doubled. During the day, the average contribution of NO_3 to α-pinene oxidation is 14% above the canopy and 35% below. Ultimately in this scenario, NO_3 is present at concentrations significant enough that it competes with OH as the second most influential daytime oxidant of α-pinene below the canopy (behind O_3). This indicates that substantial differences in ground-level chemistry may exist between forested and non-forested polluted areas.

The α-pinene oxidation rates in the Detroit scenario differ substantially from the CABINEX cases. Nighttime oxidation rates are actually smaller than in the ambient CABINEX environment, as continuous urban NO emissions reduce O_3. However, daytime oxidation rates are as large as in the polluted CABINEX case. The combined increases in the concentrations of every oxidant in the late afternoon cause α-pinene oxidation in the Detroit scenario to display a strong diel trend. While above the canopy the contribution of NO_3 is generally below 20% during the day, this contribution increases to as much as 40-50% below the canopy. Brown et al. (2005) suggested that the role of the NO_3 in monoterpene oxidation might be enhanced in areas of high BVOC oxidation rates and low-light conditions, and every model scenario confirms this hypothesis.

Isoprene oxidation is only briefly discussed, as the total rates and fractional oxidant contributions are similar across all modeled scenarios (Fig. 6). In every case, OH dominates isoprene oxidation, especially during the day when oxidation rates are most substantial. Peak below-canopy oxidation rates are generally smaller than those above, largely due to increased photolytic activity and OH concentrations above the canopy. In the polluted CABINEX scenario, NO_3 contributes up to 50% of nighttime oxidation, but during this period oxidation rates are at a minimum of <0.1 ppbv/hr. The Detroit results appear to be very similar to those from the CABINEX scenarios, supporting the notion that isoprene oxidation has relatively little dependence on NO_3 or O_3 chemistry.

3.4 First-Generation $RONO_2$ Production

Modeled differences in the oxidation rate of α-pinene (and to a smaller degree isoprene) both above and below the canopy and between scenarios suggest the possibility of correspondingly different rates of first-generation $RONO_2$ production. First-generation $RONO_2$ was given special attention because its production pathways are clearly discernible in the MCM (i.e. NO_3 + α-pinene, OH + isoprene, etc.) and because previous modeling efforts at the site have indicated that it accounts for over 80% of total $RONO_2$ for most of the day (Pratt et al., 2012).

Atmos. Chem. Phys. Discuss., doi:10.5194/acp-2016-485, 2016
Manuscript under review for journal Atmos. Chem. Phys.
Published: 14 June 2016
© Author(s) 2016. CC-BY 3.0 License.

Atmospheric Chemistry and Physics Discussions

In the ambient scenario above the canopy, OH oxidation of isoprene and subsequent reaction with NO produces the majority of daytime first-generation $RONO_2$ (~60%), while NO_3 oxidation of α-pinene provides the majority of nighttime formation (~80%), in agreement with Pratt et al. (2012) for the same location (Figs. 7 and 8). Below the canopy, α-pinene + NO_3 accounts for as much as 35% of midday production (~12:00), in contrast with only 20% above, further highlighting the impact of canopy shade. Despite the increased amount of daytime NO_3 below the canopy, the total amount of $RONO_2$ produced by NO_3 oxidation during a 24-hour period is only slightly enhanced below the canopy. This is primarily the result of similar average NO_3 concentrations in the two locations (avg. $[NO_3]$ = 0.12 pptv above and 0.13 pptv below).

In the polluted CABINEX scenario, increased NO_3 concentrations cause NO_3 oxidation of α-pinene to be a major $RONO_2$ production pathway both above and below the canopy. On average, this reaction produces 57% of above- and 63% of below-canopy first-generation $RONO_2$. While the total amount of isoprene oxidized by NO_3 is small, as shown in the previous analysis, below the canopy this reaction consistently accounts for ~20% of first-generation $RONO_2$ production. During the early afternoon (12:00-4:00), the combined oxidation of isoprene and α-pinene by NO_3 produces ~70% of first-generation $RONO_2$ below the canopy. Nearly four times as much total first-generation $RONO_2$ is produced as in the ambient scenario, and on average 89% is from NO_3 oxidation.

There are a few differences between the Detroit scenario and those previously discussed. The most notable of these is the stark difference between above- and below-canopy production of first-generation $RONO_2$. Figure 8 indicates that this difference is largely the result of increased production from NO_3 oxidation of α-pinene. During the early morning and early afternoon, the contribution of NO_3 + α-pinene below the canopy displays two strong peaks that reach values as high as 60%. The corresponding above-canopy values are consistent at ~20% during these periods. In the previous scenarios, while daytime NO_3 concentrations and the subsequent production rates of $RONO_2$ were substantially elevated below the canopy relative to above, average daily NO_3 mixing ratios were similar, leading to similar daily production totals. In Detroit however, average below canopy NO_3 concentrations are much higher than above, accounting for this difference in model results.

3.5 Secondary Organic Aerosol Production

The combination of a highly detailed chemical model and quantification of individual product partitioning allows investigation of differences in SOA production and composition between modeled scenarios. Diel plots of SOA mass loadings for each scenario are shown in Figure 9. In the ambient scenario, modeled SOA mass concentrations are in the range of ~0.3 to 1.8 μg m^{-3}. To our knowledge, the composition of ambient aerosol at UMBS has only been specified once before, and aerosol mass spectrometer measurements indicated that organic aerosol mass loadings varied from ~0.5 to 2 μg m^{-3} (Delia, 2004), in relatively good agreement with our results. Ashworth et al. (2015) modeled SOA mass loadings a factor of 4-5 lower near the ground (0.1-0.5 μg m^{-3}), with no substantial near-ground change that would be indicative of a canopy effect. Our model results indicate that more than twice as much SOA mass is produced below the canopy than above, largely due to an increase from hydroperoxide aerosol (ROOH). Very little aerosol is produced from peroxyacyl nitrates (PN) or from compounds lacking peroxide or nitrate functional groups (ROH). At the end of the model period, SOA accounts for 63% of total OA (POA + SOA)

Atmos. Chem. Phys. Discuss., doi:10.5194/acp-2016-485, 2016
Manuscript under review for journal Atmos. Chem. Phys.
Published: 14 June 2016
© Author(s) 2016. CC-BY 3.0 License.

Atmospheric Chemistry and Physics Discussions

below the canopy and only 45% above. The SOA mass yields for both isoprene (0.021-0.046) and α-pinene (0.01-0.024) agree with results from chamber experiments in which relatively little SOA forms (Carlton et al., 2009; Henry et al., 2012). The diel pattern of SOA mass loadings highlights the influence of temperature on oxidation product partitioning. Similarly to Ashworth et al. (2015), both gas- and aerosol-phase BVOC oxidation products accumulate over the course of the model run, which may result from a lack of physical loss processes. While this accumulation may lead to slight errors in the absolute values of predicted SOA mass loadings, it should have little effect on relative differences in SOA production and composition between canopy locations.

Sensitivity analyses indicate that the increased production of SOA below the canopy is largely due to the combined effects of decreased concentrations of NO and higher concentrations of isoprene (Fig. S6). Organic peroxy radicals formed from the oxidation of VOCs can react with HO_2 to form hydroperoxides, NO to generate alkoxy radicals (or $RONO_2$ to a smaller extent), NO_2 to form PN, or other RO_2 compounds to form alcohols and carbonyls (Atkinson et al., 1997; Kroll and Seinfeld, 2008). The concurrent observation of an increase in hydroperoxide aerosol below the canopy and similar $RONO_2$ aerosol levels between locations suggests that lowered NO concentrations increase the likelihood of the $RO_2 + HO_2$ reaction at the expense of $RO_2 + NO$. As a result, the production of low-volatility organic hydroperoxides is increased relative to the production of alkoxy radicals, which tend to fragment, ultimately causing increased aerosol formation. This effect has been observed in multiple chamber experiments regarding SOA formation, and it is generally found that yields are lowest in experiments where $RO_2 + NO$ dominates (Edney et al., 2005; Presto et al., 2005; Kroll et al., 2006; Kleindienst et al., 2007; Ng et al., 2007). Increased relevance of $RO_2 + HO_2$ below the canopy seems counterintuitive, as HO_x concentrations are substantially lower there than above-canopy; however, average NO concentrations are 33% lower below-canopy than above, whereas average HO_2 concentrations are only 16% lower.

Investigating the ambient scenario further, $RONO_2$ aerosol accounts for around 49% of SOA mass above the canopy and 39% below, with mass loadings in the range of approximately 0.1 to 0.5 μg m^{-3} in both environments. Mass loadings in this range agree with aerosol mass spectrometer measurements from Fry et al. (2013) performed in a Colorado front-range forest with substantial BVOC emissions and a somewhat larger anthropogenic influence (daytime O_3 ~60 ppb). It should be noted that adding a representative mix of monoterpene species to our model would serve to increase $RONO_2$ SOA yields and likely result in mass loadings somewhat larger than those measured by Fry et al. (2013). The observation of relatively similar mass loadings of aerosol-phase $RONO_2$ above and below the canopy implies that the canopy itself has a small influence on NO_3-derived aerosol production. However, that observation is a result of the fact that isoprene oxidation products compose the majority of SOA mass, as isoprene is only slightly oxidized by NO_3. From 12:00 to 18:00, over 2.5 times more NO_3-derived α-pinene $RONO_2$ aerosol is produced below the canopy than above. While the absolute amount of production through this daytime mechanism is small (~0.01 μg m^{-3}), including a mix of monoterpenes would noticeably increase the absolute difference in daytime production, as the SOA yield of other monoterpenes is substantially higher than that of α-pinene.

The ten dominant oxidation products in α-pinene and isoprene aerosol-phase $RONO_2$ are shown in Figures 10 and 11 and Tables S1 and S2. In the case of α-pinene, four or more of these products form solely through

Atmos. Chem. Phys. Discuss., doi:10.5194/acp-2016-485, 2016
Manuscript under review for journal Atmos. Chem. Phys.
Published: 14 June 2016
© Author(s) 2016. CC-BY 3.0 License.

Atmospheric Chemistry and Physics Discussions

oxidation by NO_3. A lower bound estimate of the fraction of α-pinene SOA formed from NO_3 oxidation can be made using these compounds. As a daily average, NO_3 + α-pinene produces a minimum of 25% of α-pinene SOA above the canopy and 14% below. Furthermore, this reaction is responsible for at least 74% of α-pinene $RONO_2$ SOA above the canopy and 66% below. Higher fractional contributions above the canopy are attributed to the significantly higher nighttime NO_3 concentrations there, as aerosol formation is more thermodynamically favorable at night and daily average concentrations are similar between the two environments. The distinction between α-pinene and isoprene $RONO_2$ composition is stark, as NO_3 oxidation forms the majority of α-pinene $RONO_2$, while nearly all isoprene $RONO_2$ forms through OH oxidation. This observation agrees with the fractional contributions of each oxidant to gas-phase first-generation $RONO_2$ formation.

The most noticeable difference between the ambient and artificially polluted scenarios is the ~50% reduction in total aerosol mass loadings predicted in both polluted cases (above and below the canopy). This occurs despite the fact that the total amount of isoprene oxidized is similar to the ambient case while the amount of α-pinene oxidized more than doubles. Organic nitrates constitute a much more significant fraction of total aerosol in the polluted environments (~59-61% on average), while the contribution from organic peroxides is simultaneously reduced (~14-36%). Aerosol produced from α-pinene-derived oxidation products is actually increased (~9-17%) relative to the ambient case, indicating that the primary difference between the ambient and polluted scenarios is due to a large reduction in isoprene-derived SOA. Again, RO_2 chemistry explains these observations. In the ambient case, each of the ten most prominent α-pinene and isoprene oxidation products (not necessarily $RONO_2$) in the aerosol phase contained a peroxide functional group, implying an $RO_2 + HO_2$ reaction during oxidation. While HO_x concentrations were maintained throughout the three scenarios, in the artificially polluted scenario, NO concentrations were increased by a factor of five. In a process opposite to the one described previously, this change increases the likelihood of RO production from RO_2 oxidation, reducing hydroperoxide production and thereby reducing the total amount of aerosol produced. This difference in oxidation chemistry is supported by the observation of markedly reduced isoprene and α-pinene SOA yields relative to the ambient case (0.01 or less for both α-pinene and isoprene). However, the increase in NO_3 concentrations works to offset this effect in the case of α-pinene, causing a smaller relative reduction in SOA yield than is seen for isoprene.

Despite yielding substantially less total aerosol, the polluted environment produces much more α-pinene $RONO_2$ SOA than in the ambient case (Fig. 10). Elevated NO_3 and O_3 concentrations are the primary cause of this change. The impact of increased NO_3 is exemplified by the fact that products formed solely from NO_3 + α-pinene have combined average mass loadings 36 to 100% higher (above and below, respectively) than in the ambient case. The differences between canopy environments are also more pronounced than in the ambient scenario. Virtually no NO_3-derived $RONO_2$ SOA is produced above the canopy from 10:00-18:00, whereas roughly 20% of total daily production occurs during this period below the canopy. Ultimately, NO_3-derived $RONO_2$ aerosol accounts for a minimum of 33% of total α-pinene SOA above the canopy and 26% below.

The Detroit scenario produces the least SOA of all three environments. This outcome is expected based on the previous results, as similar amounts of isoprene and α-pinene are reacted relative to the ambient case, while NO

Atmos. Chem. Phys. Discuss., doi:10.5194/acp-2016-485, 2016
Manuscript under review for journal Atmos. Chem. Phys.
Published: 14 June 2016
© Author(s) 2016. CC-BY 3.0 License.

concentrations are on average ~23 times higher than the artificially polluted case, limiting hydroperoxide production. Organic nitrates account for the overwhelming majority of total aerosol (~85-89%), further highlighting the significance of peroxy radical loss to reaction with NO. Total SOA production below the canopy is again nearly a factor of two higher than above the canopy, largely due to increases in isoprene concentrations, as isoprene oxidation products account for around 80% of total SOA mass in both environments.

While the Detroit scenario and the ambient scenario produce similar mass concentrations of α-pinene $RONO_2$ SOA, the composition of this aerosol is markedly different, denoting distinct dominant oxidation pathways in the two locations. In the ambient scenario, four out of the ten major $RONO_2$ oxidation products are formed solely through NO_3 oxidation of α-pinene, and these contribute on average as much as 74% of $RONO_2$ SOA. However, in Detroit, only three species formed solely through NO_3 + α-pinene are included in the ten dominant products, and these contribute only a minor fraction of the total (Fig. 10). Additionally, almost no $RONO_2$ is produced through daytime α-pinene + NO_3 above or below the canopy in the Detroit case. Of the ten dominant α-pinene $RONO_2$ species in Detroit, four are cross products of multiple oxidants and contribute over half of the total $RONO_2$ SOA above and below the canopy. Two of these four products, APINANO3 and APINBNO3 are formed through NO_3 oxidation followed by reaction with RO_2, or through OH oxidation and subsequent reaction with NO. In the case of initial oxidation by OH, 12-23% of the RO_2 + NO reaction will form these stable nitrates, indicating that elevated NO in Detroit largely accounts for their elevated mass loadings. However, the remaining 76-88% will form an alkoxy radical, which quickly decomposes into pinonaldehyde. In addition, NO_3-derived RO_2 that reacts with NO also produces an alkoxy radical that quickly forms pinonaldehyde. The two other dominant cross products in α-pinene $RONO_2$, C106NO3 and C98NO3, are both highly oxidized products of subsequent pinonaldehyde reaction. The mass loadings of each of these four products are therefore highly related to ambient NO levels. As a result, urban NO appears to control α-pinene oxidative processes, resulting in reduced production of $RONO_2$ SOA from NO_3 oxidation and markedly different $RONO_2$ composition than in rural environments.

4. Conclusions

A detailed 0D model was used to investigate α-pinene and isoprene oxidation chemistry and SOA production above and below a forest canopy under three scenarios. Specific focus was placed on the contribution of NO_3 to BVOC processes, as shade provided by the canopy was assumed to reduce NO_3 photolysis rates. The model accurately reproduces measured above-canopy HO_x profiles, and it responds appropriately to a sensitivity test based on steady-state NO_3 concentrations. In each of the three model scenarios, NO_3 concentrations are relatively low (<3 pptv); however, daytime concentrations are roughly twice as large below the canopy as above. Reduced photolysis frequencies are found to be the primary factor behind elevated daytime below-canopy NO_3 concentrations. The Detroit scenario displays the largest differences in NO_3 concentrations above and below the canopy, underscoring the need for further studies on the role of urban NO_3 chemistry. In accordance with NO_3 concentrations, daytime NO_3 oxidation of α-pinene below the canopy is enhanced by a factor of two or more relative to above, and in the artificially polluted scenario, NO_3 competes with OH as the second most influential daytime oxidant of α-pinene. Furthermore, the contribution of daytime NO_3 oxidation to first generation $RONO_2$ production is enhanced below

Atmos. Chem. Phys. Discuss., doi:10.5194/acp-2016-485, 2016
Manuscript under review for journal Atmos. Chem. Phys.
Published: 14 June 2016
© Author(s) 2016. CC-BY 3.0 License.

Atmospheric Chemistry and Physics Discussions

the canopy in every case. In the artificially polluted case specifically, NO_3 + VOCs produce over 80% of first-generation $RONO_2$ for nearly the entire diel period. While SOA production is relatively small in every environment studied, total production is increased below the canopy in every case. Additionally, below-canopy daytime production of NO_3-derived α-pinene $RONO_2$ SOA is greater than that above the canopy by a factor of two or more. However, the total difference in NO_3-derived SOA production between canopy locations is small due to the use of α-pinene as the only monoterpene, suggesting a need for future modeling incorporating both detailed chemistry and a more comprehensive suite of BVOCs. The relative concentrations of HO_x and NO substantially affect both the composition and total production of SOA, as changes in the relative ratio of HO_2 to NO result in different dominant RO_2 reaction pathways. Ultimately, the results of this study indicate that neglecting differences between below-canopy and above-canopy environments can lead to incorrect assumptions about NO_3 oxidation rates, $RONO_2$ production, and SOA production and composition. However, the implications of such assumptions vary based on the specific location being considered. Future work will look to improve the model by including both transport mechanisms and a range of representative monoterpene species.

Atmos. Chem. Phys. Discuss., doi:10.5194/acp-2016-485, 2016
Manuscript under review for journal Atmos. Chem. Phys.
Published: 14 June 2016
© Author(s) 2016. CC-BY 3.0 License.

Atmospheric Chemistry and Physics Discussions

Copyright Statement:

Authors grant Copernicus Publications a licence to publish the article and identify itself as the original publisher.

Authors grant Copernicus Publications commercial rights to produce hardcopy volumes of the journal for purchase by libraries and individuals.

Authors grant any third party the right to use the article freely under the stipulation that the original authors are given credit and the appropriate citation details are mentioned.

The article is distributed under the Creative Commons Attribution 3.0 License. Unless otherwise stated, associated published material is distributed under the same licence.

Code Availability:

The MATLAB code associated with this manuscript is available upon request.

Data Availability:

The compiled datasets used to produce each figure within this manuscript are available as Igor Pro files upon request.

Author Contribution:

B.C. Schulze developed the model, performed simulations and data analysis, and wrote the manuscript. H.W. Wallace and R.J. Griffin assisted heavily with model development, data analysis, and manuscript editing. H.W. Wallace, J. H. Flynn, B.L. Lefer, M.H. Erickson, B.T. Jobson, S. Dusanter, S.M. Griffith, R.F. Hansen, and P.S. Stevens performed atmospheric measurements during CABINEX that were used as model inputs. J.H. Flynn, P.S. Stevens, S. Dusanter, S.M. Griffith, and R.F. Hansen provided helpful comments and edits.

Acknowledgements:

We would like to acknowledge the National Science Foundation for funding this work with grant numbers AGS-0904214 and AGS-0904167.

Atmos. Chem. Phys. Discuss., doi:10.5194/acp-2016-485, 2016
Manuscript under review for journal Atmos. Chem. Phys.
Published: 14 June 2016
© Author(s) 2016. CC-BY 3.0 License.

Atmospheric Chemistry and Physics Discussions

References

Arneth, A., Schurgers, G., Lathiere, J., Duhl, T., Beerling, D. J., Hewitt, C. N., Martin, M., and Guenther, A.: Global terrestrial isoprene emission models: sensitivity to variability in climate and vegetation, Atmos. Chem. Phys., 11, 8037–8052, doi:10.5194/acp-11-8037-2011, 2011.

Ashworth, K., Chung, S. H., Griffin, R. J., Chen, J., Forkel, R., Bryan, A. M., and Steiner, A. L.: FORest Canopy Atmosphere Transfer (FORCAsT) 1.0: a 1-D model of biosphere-atmosphere chemical exchange, Geosci. Model Dev., 8, 3765-3784, doi:10.5194/gmd-8-3765-2015, 2015.

Atkinson, R.: Gas-Phase Tropospheric Chemistry of Volatile Organic Compounds: 1. Alkanes and Alkenes, J. Phys. Chem. Ref. Data, 26, 215-290, doi:10.1063/1.556012, 1997.

Atkinson, R. and Arey, J.: Atmospheric Degradation of Volatile Organic Compounds, Chem. Rev., 103, 4605-4638, 2003.

Ayres, B. R., Allen, H. M., Draper, D. C., Brown, S. S., Wild, R. J., Jimenez, J. L., Day, D. A., Campuzano-Jost, P., Hu, W., de Gouw, J., Koss, A., Cohen, R. C., Duffey, K. C., Romer, P., Baumann, K., Edgerton, E., Takahama, S., Thornton, J. A., Lee, B. H., Lopez-Hilfiker, F. D., Mohr, C., Wennberg, P. O., Nguyen, T. B., Teng, A., Goldstein, A. H., Olson, K., and Fry, J. L.: Organic nitrate aerosol formation via NO_3 + biogenic volatile organic compounds in the southeastern United States, Atmos. Chem. Phys., 15, 13377-13392, doi:10.5194/acp-15-13377-2015, 2015.

Bey, I., Aumont, B. and Toupance, G.: The nighttime production of OH radicals in the continental troposphere, Geophys. Res. Lett., 24, 1067-1070, doi:10.1029/97GL00889, 1997.

Brown, S. S. and Stutz, J.: Nighttime radical observations and chemistry, Chem. Soc. Rev., 41, 6405–6447, doi:10.1039/c2cs35181a, 2012.

Brown, S.S., Osthoff, H.D., Stark, H., Dubé, W.P., Ryerson, T.B., Warneke, C., de Gouw, J.A., Wollny, A.G., Parrish, D.D., Fehsenfeld, F.C., and Ravishankara, A.R.: Aircraft observations of daytime NO_3 and N_2O_5 and their implications for tropospheric chemistry. J. Photochem. Photobiol. A Chem., 176, 270–278, doi:10.1016/j.jphotochem.2005.10.004, 2005.

Brown, S. S., Dubé, W. P., Peischl, J., Ryerson, T. B., Atlas, E., Warneke, C., de Douw, J. A., Hekkert, S. T. L., Brock, C. A., Flocke, F., Trainer, M., Parrish, D. D., Feshenfeld, F., and Ravishankara, A. R.: Budgets for nocturnal VOC oxidation by nitrate radicals aloft during the 2006 Texas Air Quality Study, J. Geophys. Res., 116, D24305, doi:10.1029/2011JD016544, 2011.

Bryan, A. M., Bertmann, S. B., Carroll, M. A., Dusanter, S., Edwards, G. D., Forkel, R., Griffith, S., Guenther, A. B., Hansen, R. F., Helmig, D., Jobston, B. T., Keutsch, F. N., Lefer, B. L., Pressley, S. N., Shepson, P. B., Stevens, P. S., and Steiner, A. L.: In-canopy gas-phase chemistry during CABINEX 2009: sensitivity of a 1-D canopy model to vertical mixing and isoprene chemistry, Atmos. Chem. Phys., 12, 8829-8849, doi:10.5194/acp-12-8829-2012, 2012.

Carlton, A. G., Wiedinmyer, C., and Kroll, J. H.: A review of Secondary Organic Aerosol (SOA) formation from isoprene, Atmos. Chem. Phys., 9, 4987-5005, doi:10.5194/acp-9-4987-2009, 2009.

Carroll, M. A., Bertman, S. B. and Shepson, P. B.: Overview of the Program for Research on Oxidants: Photochemistry, Emissions, and Transport (PROPHET) summer 1998 measurements intensive, J. Geophys. Res., 106, 275-288, doi:10.1029/2001JD900189, 2001.

Carslaw, N., Creasey, D. J., Harrison, D., Heard, D. E., Hunter, M. C., Jacobs, P. J., Jenkin, M. E., Lee, J. D., Lewis, A. C., Pilling, M. J., Saunders, S. M., and Seakins, P.W.: OH and HO_2 radical

© Author(s) 2016. CC-BY 3.0 License.

chemistry in a forested region of north-western Greece, Atmos. Environ., 35, 4725–4737, doi:10.1016/S1352-2310(01)00089-9, 2001.

Colville, C. J., and Griffin, R. J.: The roles of individual oxidants in secondary organic aerosol formation from Δ^3-carene: 2. soa formation and oxidant contribution, Atmos. Environ., 38, 4013-4023, doi:10.1016/j.atmosenv.2004.03.063, 2004.

Cooper, O.R., Moody, J.L., Thornberry, T.D., Town, M.S., and Carroll, M.A.: PROPHET 1998 meteorological overview and air-mass classification, J. Geophys. Res. 106, 24,289-24,299, doi:10.1029/2000JD900409, 2001.

Delia, A.: Real-Time Measurements of Non-Refractory Particle Composition and Interactions at Rural and Semi-Rural Sites, PhD Thesis, University of Colorado-Boulder, 2004.

Edney, E. O., Kleindiest, T. E., Jaoui, M., Lewandowski, M., Offenberg, J. H., Wang, W., and Claeys, M.: Formation of 2-methyl tetrols and 2-methylglyceric acid in secondary organic aerosol from laboratory irradiated isoprene/NO_x/SO_2/air mixtures and their detection in ambient $PM_{2.5}$ samples collected in the eastern United States, Atmos. Environ., 39, 5281-5289, 2005.

Farmer, D. K., Perring, A. E., Wooldridge, P. J., Blake, D. R., Baker, A., Meinardi, S., Huey, L. G., Tanner, D., Vargas, O. and Cohen, R. C.: Impact of organic nitrates on urban ozone production, Atmos. Chem. Phys., 11, 4085-4094, doi:10.5194/acp-11-4085-2011, 2011.

Flynn, J., Lefer, B., Rappengluck, B., Leuchner, M., Perna, R., Dibb, J., Ziemba, L., Anderson, C., Stutz, J., Brune, W., Ren, X. R., Mao, J. Q., Luke, W., Olson, J., Chen, G., and Crawford, J.: Impact of clouds and aerosols on ozone production in Southeast Texas, Atmos. Environ., 44, 4126–4133, doi:10.1016/j.atmosenv.2009.09.005, 2010.

Fry, J. L., Kiendler-Scharr, A., Rollins, A. W., Wooldridge, P. J., Brown, S. S., Fuchs, H., Dubé, W., Mensah, A., dal Maso, M., Tillmann, R., Dorn, H.-P., Brauers, T., and Cohen, R. C.: Organic nitrate and secondary organic aerosol yield from NO_3 oxidation of β-pinene evaluated using a gas-phase kinetics/aerosol partitioning model, Atmos. Chem. Phys., 9, 1431–1449, doi:10.5194/acp-9-1431-2009, 2009.

Fry, J. L., Kiendler-Scharr, A., Rollings, A. W., Brauers, T., Brown, S. S., Dorn, H.-P., Dubé, W. P., Fuchs, H., Mensah, A., Rohrer, F., Tillmann, R., Wahner, A., Wooldridge, P. J., and Cohen, R. C.: SOA from limonene: role of NO_3 in its generation and degradation, Atmos. Chem. Phys., 11, 3879-3894, doi:10.5194/acp-11-3879-2011, 2011.

Fry, J. L., Draper, D. C., Zarzana, K. J., Campuzano-Jost, P., Day, D. A., Jimenez, J. L., Brown, S. S., Cohen, R. C., Kaser, L., Hansel, A., Cappellin, L., Karl, T., Hodzie Roux, A., Turnipseed, A., Cantrell, C., Lefer, B. L., and Grossberg, N.: Observations of gas- and aerosol-phase organic nitrates at BEACHON-RoMBAS 2011, Atmos. Chem. Phys., 13, 8585-8605, doi:10.5194/acp-13-8585-2013, 2013.

Fry, J. L., Draper, D. C., Barsanti, K. C., Smith, J. N., Ortega, J., Winkler, P. M., Lawler, M. J., Brown, S. S., Edwards, P. M., Cohen, R. C., and Lee, L.: Secondary Organic Aerosol Formation and Organic Nitrate Yield from NO_3 Oxidation of Biogenic Hydrocarbons, Environ. Sci. Technol., 48, 11944-11953, doi:10.1021/es502204x, 2014.

Fuchs, H., Bohn, B., Hofzumahaus, A., Holland, F., Lu, K. D., Nehr, S., Rohrer, F. and Wahner, A.: Detection of HO2 by laser-induced fluorescence: calibration and interferences from RO2 radicals, Atmos. Meas. Tech., 4, 1209-1225, doi:10.5194/amt-4-1209-2011, 2011.

© Author(s) 2016. CC-BY 3.0 License.

Fuentes, J. D., Wang, D., Bowling, D. R., Potosnak, M., Monson, R.K., Goliff, W. S., and Stockwell, W. R.: Biogenic Hydrocarbon Chemistry within and Above a Mixed Deciduous Forest, J. Atmos. Chem., 56, 165-185, doi:10.1007/s10874-006-9048-4, 2006.

Geyer, A., Alicke, B., Ackermann, R., Martinez, M., Harder, H., Brune, W., di Carlo, P., Williams, E., Jobson, T., Hall, S., Shetter, R., and Stutz, J.: Direct observations of daytime NO_3: implications for urban boundary layer chemistry. J. Geophys. Res., 108, 4368, doi:10.1029/2002JD002967, 2003a.

Geyer, A., Bachmann, K., Hofzumahaus, A., Holland, F., Konrad, S., Klupfel, T., Patz, H.-W., Perner, D., Mihelcic, D., Schafer, H.-J., Volz-Thomas, A. and Platt, U.: Nighttime formation of peroxy and hydroxyl radicals during the BERLIOZ campaign: Observations and modeling studies, J. Geophys. Res., 108, 4, 8249, doi:10.1029/2001JD000656, 2003b.

Golz, C., Senzig, J., and Platt, U.: NO_3-initiated oxidation of biogenic hydrocarbons, Chemosphere – Global Change Science, 3, 339-352, doi:10.1016/S1465-9972(01)00015-0, 2001.

Griffith, S. M., Hansen, R. F., Dusanter, S., Stevens, P. S., Alaghmand, M., Bertman, S. B., Carroll, M. A., Erickson, M., Galloway, M., Grossberg, N., Hottle, J., Hou, J., Jobson, B. T., Kammrath, A., Keutsch, F. N., Lefer, B. L., Mielke, L. H., O'Brien, A., Shepson, P. B., Thurlow, M., Wallace, W., Zhang, N., and Zhou, X. L.: OH and HO_2 radical chemistry during PROPHET 2008 and CABINEX 2009 – Part 1: Measurements and model comparison, Atmos. Chem. Phys., 13, 5403-5423, doi:10.5194/acp-13-5403-2013, 2013.

Guenther, A., Hewitt, C., Erickson, D., Fall, R., Geron, C., Graedel, T., Harley, P., Klinger, L., Lerdau, M., McKay, W. A., Pierce, T., Scholes, B., Steinbrecher, R., Tallamraju, R., Taylor, J., and Zimmerman, P.: A global model of natural volatile organic compound emissions, J. Geophys. Res., 100, 8873–8892, doi:10.1029/94JD02950, 1995.

Guenther, A. B., Jiang, X., Heald, C. L., Sakulyanontvittaya, T., Duhl, T., Emmons, L. K., and Wang, X.: The Model of Emissions of Gases and Aerosols from Nature version 2.1 (MEGAN2.1): an extended and updated framework for modeling biogenic emissions, Geosci. Model Dev., 5, 1471–1492, doi:10.5194/gmd-5- 1471-2012, 2012.

Hallquist, M., Wängberg, I., Ljungstrom, E., Barnes, I., and Becker, K. H.: Aerosol and Product Yields from NO_3 Radical-Initiated Oxidation of Selected Monoterpenes, Environ. Sci. Technol., 33, 553–559, doi:10.1021/es980292s, 1999.

Hallquist, M., Wenger, J. C., Baltensperger, U., Rudich, Y., Simpson, D., Claeys, M., Dommen, J., Donahue, N. M., George, C., Goldstein, A. H., Hamilton, J. F., Herrmann, H., Hoffmann, T., Iinuma, Y., Jang, M., Jenkin, M. E., Jimenez, J. L., Kiendler-Scharr, A., Maenhaut, W., McFiggans, G., Mentel, Th. F., Monod, A., Prevot, A. S. H., Seinfeld, J. H., Surratt, J. D., Szmigielski, R., and J. Wildt: The formation, properties and impact of secondary organic aerosol: current and emerging issues, Atmos. Chem. Phys. 9, 5155–5236, doi:10.5194/acp-9-5155-2009, 2009.

Hansen, R. F., Griffith, S., Dusanter, S., Rickly, P., Stevens, P. S., Bertman, S. B., Carroll, M. A., Erickson, M. H., Flynn, J. H., Grossberg, N., Jobson, B. T., Lefer, B. L., and Wallace, W. H.: Total hydroxyl radical reactivity during CABINEX 2009 - Part 1: Field measurements. Atmos. Chem. Phys., 14, 2923–2937, doi:10.5194/acp-14-2923-2014, 2014.

Heald, C. L., Jacob, D. J., Park, R. J., Russell, L. M., Huebert, B. J., Seinfeld, J. H., Liao, H., and Weber, R. J.: A large organic aerosol source in the free troposphere missing from current models, Geophys. Res. Lett., 32, L18809, doi:10.1029/2005GL023831, 2005.

© Author(s) 2016. CC-BY 3.0 License.

Henry, K. M. and Donahue, N. M.: Photochemical Aging of α-Pinene Secondary Organic Aerosol: Effects of OH Radical Sources and Photolysis, J. Phys. Chem. A, 116, 5932–5940, doi:10.1021/jp210288s, 2012.

Jenkin, M. E., Saunders, S. M., and Pilling, M. J.: The tropospheric degradation of volatile organic compounds: a protocol for mechanism development, Atmos. Environ., 31, 81-104, doi:10.1016/S1352-2310(96)00105-7, 1997.

Jimenez, J. L., Canagaratna, M. R., Donahue, N. M., Prevot, A. S. H., Zhang, Q., Kroll, J. H., DeCarlo, P. F., Allan, J. D., Coe, H., Ng, N. L., Aiken, A. C., Docherty, K. S., Ulbrich, I. M., Grieshop, A. P., Robinson, A. L., Duplissy, J., Smith, J. D., Wilson, K. R., Lanz, V. A., Hueglin, C., Sun, Y. L., Tian, J., Laaksonen, A., Raatikainen, T., Rautiainen, J., Vaattovaara, P., Ehn, M., Kulmala, M., Tomlinson, J. M., Collins, D. R., Cubison, M. J., Dunlea, E. J., Huffman, J. A., Onasch, T. B., Alfarra, M. R., Williams, P. I., Bower, K., Kondo, Y., Schneider, J., Drewnick, F., Borrmann, S., Weimer, S., Demerjian, K., Salcedo, D., Cottrell, L., Griffin, R., Takami, A., Miyoshi, T., Hatakeyama, S., Shimono, A., Sun, J. Y., Zhang, Y. M., Dzepina, K., Kimmel, J. R., Sueper, D., Jayne, J. T., Herndon, S. C., Trimborn, A. M., Williams, L. R., Wood, E. C., Middlebrook, A. M., Kolb, C. E., Baltensperger, U., and Worsnop, D. R.: Evolution of Organic Aerosols in the Atmosphere, Science, 326, 1525–1529, doi:10.1126/science.1180353, 2009.

Kim, S., Guenther, A., Karl, T., and Greenberg, J.: Contributions of primary and secondary biogenic VOC to total OH reactivity during the CABINEX (Community Atmosphere-Biosphere INteractions Experiments)-09 field campaign, Atmos. Chem. Phys., 11, 8613-8623, doi:10.5194/acp-11-8613-2011, 2011.

Kleindienst, T. E., Lewandowski, M., Offenberg, J. H., Jaoui, M., and Edney, E. O.: Ozone-isoprene reaction: Re-examination of the formation of secondary organic aerosol, Geophys. Res. Lett., 34, L01805, doi:10.1029/2006GL027485, 2007.

Kroll, J.H. and J.H. Seinfeld: Chemistry of secondary organic aerosol: Formation and evolution of low-volatility organics in the atmosphere, Atmos. Environ. 42, 3593–3624, doi:10.1016/j.atmosenv.2008.01.003, 2008.

Kroll, J. H., Ng, N. L., Murphy, S. M., Flagan, R. C., and Seinfeld, J. H.; Secondary Organic Aerosol Formation from Isoprene Photooxidation, Environ. Sci. Technol., 40, 1869-1877, doi:10.1021/es0524301, 2006.

Lelieveld, J., Butler, T. M., Crowley, J. N., Dillon, T. J., Fischer, H., Ganzeveld, L., Harder, H., Lawrence, M. G., Martinez, M., Taraborrelli, D., and Williams, J.: Atmospheric oxidation capacity sustained by a tropical forest, Nature, 452, 737–740, doi:10.1038/nature06870, 2008.

Lee, B. H., Mohr, C. Lopez-Hilfiker, F. D., Lutz, A., Hallquist, M., Lee, L., Romer, P., Cohen, R. C., Iyer, S., Kurten, T., Hu, W., Day, D. A., Campuzano-Jost, P., Jimenez, J. L., Xu, L., Ng. N. L., Guo, H., Weber, R. J., Wild, R. J., Brown, S. S., Koss, A., de Gouw, J., Olson, K., Goldstein, A. H., Seco, R., Kim, S., McAvey, K., Shepson, P. B., Starn, T., Baumann, K., Edgerton, E. S., Liu, J., Shilling, J. E., Miller, D. O., Brune, W., Schobesberger, S., D'Ambro, E. L., and Thornton, J. A.: Highly functionalized organic nitrates in the southeast United States: Contribution to secondary organic aerosol and reactive nitrogen budgets, Proceedings of the National Academy of Sciences, 113, 1516-1521, doi:10.1073/pnas.1508108113, 2016

Matsumoto, J., Imai, H., Kosugi, N., and Kaji, Y.: In situ measurement of N2O5 in the urban atmosphere by thermal decomposition/laser-induced fluorescence technique, Atmos. Environ., 39, 6802–6811, 2005.

Mihele, C. M. and Hastie, D. R.: Radical chemistry at a forested continental site: Results from the PROPHET 1997 campaign, J. Geophys. Res., 108, 4450, doi: 10.1029/2002jd002888, 2003.

© Author(s) 2016. CC-BY 3.0 License.

Mogensen, D., Gierens, R., Crowley, J. N., Keronen, P., Smolander, S., Sogachev, A., Nolscher, A. C., Zhou, L., Kulmala, M., Tang, M. J., Williams, J. and Boy, M.: Simulations of atmospheric OH, O_3, and NO_3 reactivities within and above the boreal forest, Atmos. Chem. Phys., 15, 3909-3932, doi:10.5194/acp-15-3909-2015, 2015.

Monks, Paul: Gas-phase radical chemistry in the troposphere, Chem. Soc. Rev., 34, 376–395, doi:10.1039/b307982c, 2005.

National Center for Atmospheric Research (NCAR), Tropospheric Ultraviolet and Visible Radiation Model (TUV), http://cprm.acom.ucar.edu/Models/TUV/Interactive_TUV/, (Accessed May 2016).

Ng, N. L., Kroll, J. H., Chan, A. W. H., Chhabra, P. S., Flagan, R. C., and Seinfeld, J. H.: Secondary organic aerosol formation from m-xylene, toluene, and benzene, Atmos. Chem. Phys., 7, 3909-3922, 2007.

Noxon, J. F., Norton, R. B., and Marovich, E.: NO_3 in the troposphere, J. Geophys. Res. 7, 125-128, doi:10.1029/GL007i002p00125, 1980.

Odum, J. R., Hoffmann, T., Bowman, F., Collins, D., Flagan, R.C., and Seinfeld, J.H.: Gas/Particle Partitioning and Secondary Organic Aerosol Yields, Environ. Sci. Technol., 30, 2580–2585, doi:10.1021/es950943+, 1996.

Ortega, J., Helmig, D., Guenther, A., Harley, P., Pressley, S., and Vogel, C.: Flux estimates and OH reaction potential of reactive biogenic volatile organic compounds (BVOCs) from a mixed northern hardwood forest, Atmos. Environ., 41, 5479-5495, doi:10.1016/j.atmosenv.2006.12.033, 2007.

Pankow, J. F.: An absorption model of the gas/aerosol partitioning of organic compounds in the atmosphere, Atmos. Environ., 28, 185–188, 1994a.

Pankow, J. F.: An absorption model of the gas/aerosol partitioning involved in the formation of secondary organic aerosol, Atmos. Environ., 28, 189–193, 1994b.

Pankow, J. F., and Asher, W. E.: SIMPOL.1: a simple group contribution method for predicting vapor pressures and enthalpies of vaporization of multifunctional organic compounds, Atmos. Chem. Phys., 8, 2773-2796, doi:10.5194/acp-8-2773-2008, 2008.

Paulot, F., Henze, D. K., and Wennberg, P. O.: Impact of the isoprene photochemical cascade on tropical ozone, Atmos. Chem. Phys., 12, 1307-1325, doi:10.5194/acp-12-1307-2012, 2012

Pratt, K. A., Mielke, L. H., Shepson, P. B., Bryan, A. M., Steiner, A. L., Ortega, J., Daly, R., Helmig, D., Vogel, C. S., Griffith, S., Dusanter, S., Stevens, P. S., and Alaghmand, M.: Contributions of individual reactive biogenic volatile organic compounds to organic nitrates above a mixed forest, Atmos. Chem. Phys., 12, 10125–10143, doi:10.5194/acp-12-10125-2012, 2012.

Presto, A. A., Hartz, K. E. H., and Donahue, N. M.: Secondary organic aerosol production from terpene ozonolysis. 2. Effect of NO_x concentration, Environ, Sci. Technol., 39, 7046-7054, 2005.

Pugh, T. A. M., MacKenzie, A. R., Hewitt, C. N., Langford, B., Edwards, P. M., Furneaux, K. L., Heard, D. E., Hopkins, J. R., Jones, C. E., Karunaharan, A., Lee, J., Mills, G., Misztal, P., Moller, S., Monks, P. S., and Whalley, L. K.: Simulating atmospheric composition over a South-East Asian tropical rainforest: Performance of a chemistry box model, Atmos. Chem. Phys., 10, 279–298, doi:10.5194/acp-10-279-2010, 2010.

© Author(s) 2016. CC-BY 3.0 License.

Pye, H.O.T. and Seinfeld, J.H.: A global perspective on aerosol from low-volatility organic compounds, Atmos. Chem. Phys., 10, 4377–4401, doi:10.5194/acp-10-4377-2010, 2010.

Ren, X., Brune, W. H., Mao, J., Mitchell, M. J., Lesher, R. L., Simpas, J. B., Metcalf, A. R., Schwab, J. J., Cai, C., Li, Y., Demerjian, K. L., Felton, H. D., Boynton, G., Adams, A., Perry, J., He, Y., Zhou, X., and Hou, J.: Behavior of OH and HO_2 in the winter atmosphere in New York City, Atmos. Environ., 40,S252-S263, 2006.

Rinne, J., Markkanen, T., Ruuskanen, T. M., Petaja, T., Keronen, P., Tang, M. J., Crowley, J. N., Rannik, U., and Vesala, T.: Effect of chemical degradation on fluxes of reactive compounds – a study with a stochastic Lagrangian transport model, Atmos. Chem. Phys., 12, 4843-4854, doi:10.5194/acp-12-4843-2012, 2012.

Rollins, A. W., Pusede, S., Wooldridge, P., Min, K.-E., Gentner, D. R., Goldstein, A. H., Liu, S., Day, D. A., Russell, L. M., Rubitschun, C. L., Surratt, J. D., and Cohen, R. C.: Gas/particle partitioning of total alkyl nitrates observed with TD-LIF in Bakersfield, J. Geophys. Res., 118, 6651-6662, doi:10.1002/jgrd.50522, 2013.

Saunders, S. M., Jenkin, M. E., Derwent, R. G., and Pilling, M. J.: Protocol for the development of the Master Chemical Mechanism, MCM v3 (Part A): tropospheric degradation of non-aromatic volatile organic compounds, Atmos. Chem. Phys., 3, 161-180, doi:10.5194/acp-3-161-2003, 2003.

Seinfeld, J. H. and Pankow, J. F.: Organic Atmospheric Particulate Material, Annu. Rev. Phys. Chem., 54:121-40, doi:10.1146/annurev.physchem.54.011002.103756, 2003.

Seok, B., Helmig, D., Ganzeveld, L., Williams, M. W., and Vogel, C. S.: Dynamics of nitrogen oxides and ozone above and within a mixed hardwood forest in northern Michigan, Atmos. Chem. Phys., 13, 7301-7320, doi:10.5194/acp-13-7301-2013, 2013.

Stavrakou, T., Peeters, J., and Müller, J.-F.: Improved global modelling of HO_x recycling in isoprene oxidation: evaluation against the GABRIEL and INTEX-A aircraft campaign measurements, Atmos. Chem. Phys., 10, 9863–9878, doi:10.5194/acp-10-9863-2010, 2010.

Stutz, J., Wong, K. W., Lawrence, L., Ziemba, L., Flynn, J. H., Rappengluck, B., and Lefer, B.: Nocturnal NO_3 radical chemistry in Houston, TX, Atmos. Environ., 44, 4099–4106, doi:10.1016/j.atmosenv.2009.03.004, 2010.

VanReken, T. M., Mwaniki, G. R., Wallace, H. W., Pressley, S. N., Erickson, M. H., Jobson, B. T., and Lamb, B. K.: Influence of air mass origin on aerosol properties at a remote Michigan forest site, Atmos. Environ., 107, 35–43, doi:10.1016/j.atmosenv.2015.02.027, 2015.

Volkamer, R., Jimenez, J. L., Martini, F. S., Dzepina, K., Zhang, Q., Salcedo, D., Molina, L. T., Worsnop, D. R., and Molina, M. J.: Secondary organic aerosol formation from anthropogenic air pollution: Rapid and higher than expected, Geophys. Res. Lett., 33, L17811, doi:10.1029/2006GL026899, 2006.

Wallace, H. W.: Experimental Observations of Non-Methane Hydrocarbons and NO_x Sources in Urban and Rural Locations, PhD Thesis, Washington State University, 2013.

Winer, A. M., Atkinson, R., and Pitts, J. N. J.: Gaseous Nitrate Radical: Possible Nighttime Atmospheric Sink for Biogenic Organic Compounds, Science, 224, 156–159, doi:10.1126/science.224.4645.156, 1984.

Wolfe, G. M., Thornton, J. A., Bouvier-Brown, N. C., Goldstein, A. H., Park, J.-H., McKay, M., Matross, D. M., Mao, J., Brune, W. H., LaFranchi, B. W., Browne, E. C., Min, K.-E., Wooldridge, P. J., Cohen, R.C., Crounse, J. D., Faloona, I. C., Gilman, J. B., Kuster, W. C., de Gouw, J. A.,

© Author(s) 2016. CC-BY 3.0 License.

Huisman, A., and Keutsch, F. N.: The Chemistry of Atmosphere-Forest Exchange (CAFE) Model – Part 2: Application to BEARPEX-2007 observations, Atmos. Chem. Phys., 11, 1269-1294, doi:10.5194/acp-11-1269-2011, 2011.

Wu, S. L., Mickley, L. J., Jacob, D. J., Logan, J. A., Yantosca, R. M., and Rind, D.: Why are there such large differences between models in global budgets of tropospheric ozone?, J. Geophys. Res., 112, D05302, doi:10.1029/2006JD007801, 2007.

Xu, L., Guo, H., Boyd, C. H., Klein, M., Bougiatioti, A., Cerully, K. M., Hite, J. R., Isaacman-Van Wertz, G., Kreisberg, N. M., Knote, C., Olson, K., Koss, A., Goldstein, A. H., Hering, S. V., Gouw, J. D., Baumann, K., Lee, S. H., Nenes, A., Weber, R. J., and Ng, N. L.: Effects of Anthropogenic Emissions on Aerosol Formation from Isoprene and Monoterpenes in the Southeastern United States, Proceedings of the National Academy of Sciences, doi:10.1073/pnas.1417609112, 2014.

Xu, L., Suresh, S., Guo, H., Weber, R. J., and Ng, N. L.: Aerosol characterization over the southeastern United States using highresolution aerosol mass spectrometry: spatial and seasonal variation of aerosol composition and sources with a focus on organic nitrates, Atmos. Chem. Phys., 15, 7307–7336, doi:10.5194/acp-15-7307-2015, 2015.

Zhang, Q., Jimenez, J. L., Canagaratna, M. R., Allan, J. D., Coe, H., Ulbrich, I., Alfarra, M. R., Takami, A., Middlebrook, A. M., Sun, Y. L., Dzepina, K., Dunlea, E., Docherty, K., DeCarlo, P. F., Salcedo, D., Onasch, T., Jayne, J. T., Miyoshi, T., Shimono, A., Hatakeyama, S., Takegawa, N., Kondo, Y., Schneider, J., Drewnick, F., Borrmann, S., Weimer, S., Demerjian, K., Williams, P., Bower, K., Bahreini, R., Cottrell, L., Griffin, R. J., Rautiainen, J., Sun, J. Y., Zhang, Y. M., and Worsnop, D. R.: Ubiquity and dominance of oxygenated species in organic aerosols in anthropogenically-influenced Northern Hemisphere midlatitudes, Geophys. Res. Lett., 34, L13801, doi:10.1029/2007GL029979, 2007.

Zhao, D. F., Kaminski, M., Schlag, P., Fuchs, H., Acir, I.-H., Bohn, B., Häseler, R., Kiendler-Scharr, A., Rohrer, F., Tillmann, R., Wang, M. J., Wegener, R., Wildt, J., Wahner, A., and Mentel, Th. F.: Secondary organic aerosol formation from hydroxyl radical oxidation and ozonolysis of monoterpenes, Atmos. Chem. Phys., 15, 991-1012, doi:10.5194/acp-15-991-2015,

Atmos. Chem. Phys. Discuss., doi:10.5194/acp-2016-485, 2016
Manuscript under review for journal Atmos. Chem. Phys.
Published: 14 June 2016
© Author(s) 2016. CC-BY 3.0 License.

Atmospheric Chemistry and Physics Discussions

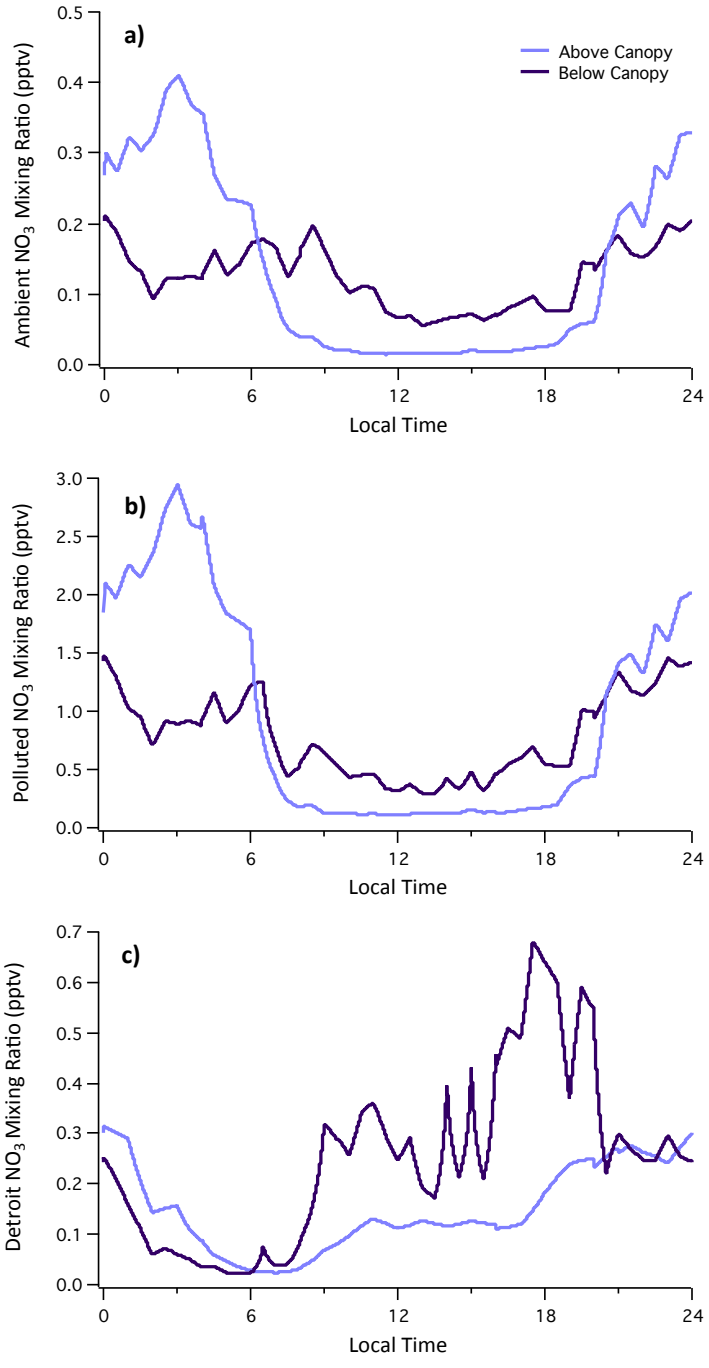

Figure 1. Modeled NO_3 mixing ratios (pptv) for (**a**) the ambient CABINEX scenario; (**b**) the artificially polluted scenario; (**c**) the Detroit scenario.

Atmos. Chem. Phys. Discuss., doi:10.5194/acp-2016-485, 2016
Manuscript under review for journal Atmos. Chem. Phys.
Published: 14 June 2016
© Author(s) 2016. CC-BY 3.0 License.

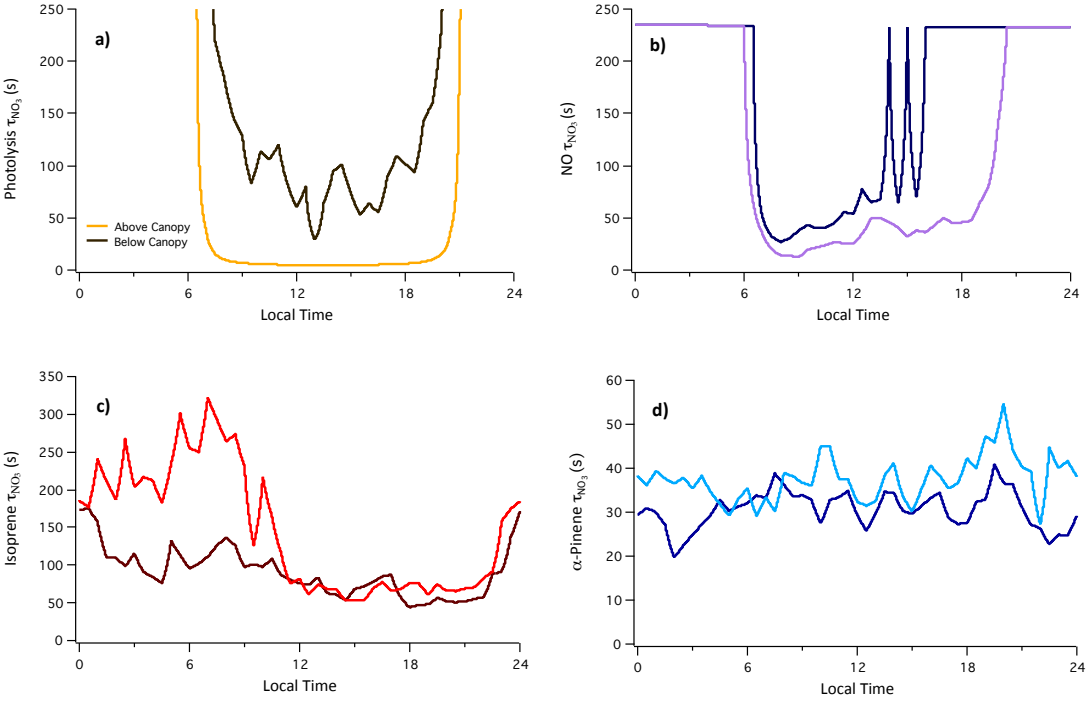

Figure 2. Modeled lifetime of NO_3 (s) with respect to (**a**) photolysis; (**b**) reaction with NO; (**c**) oxidation of isoprene; (**d**) oxidation of α-pinene. As median measured nighttime NO mixing ratios were typically below the detection limit of the instrument, NO mixing ratios were held at the detection limit during these periods for modeling purposes, leading to a constant lifetime value in (**b**) at night.

Atmos. Chem. Phys. Discuss., doi:10.5194/acp-2016-485, 2016
Manuscript under review for journal Atmos. Chem. Phys.
Published: 14 June 2016
© Author(s) 2016. CC-BY 3.0 License.

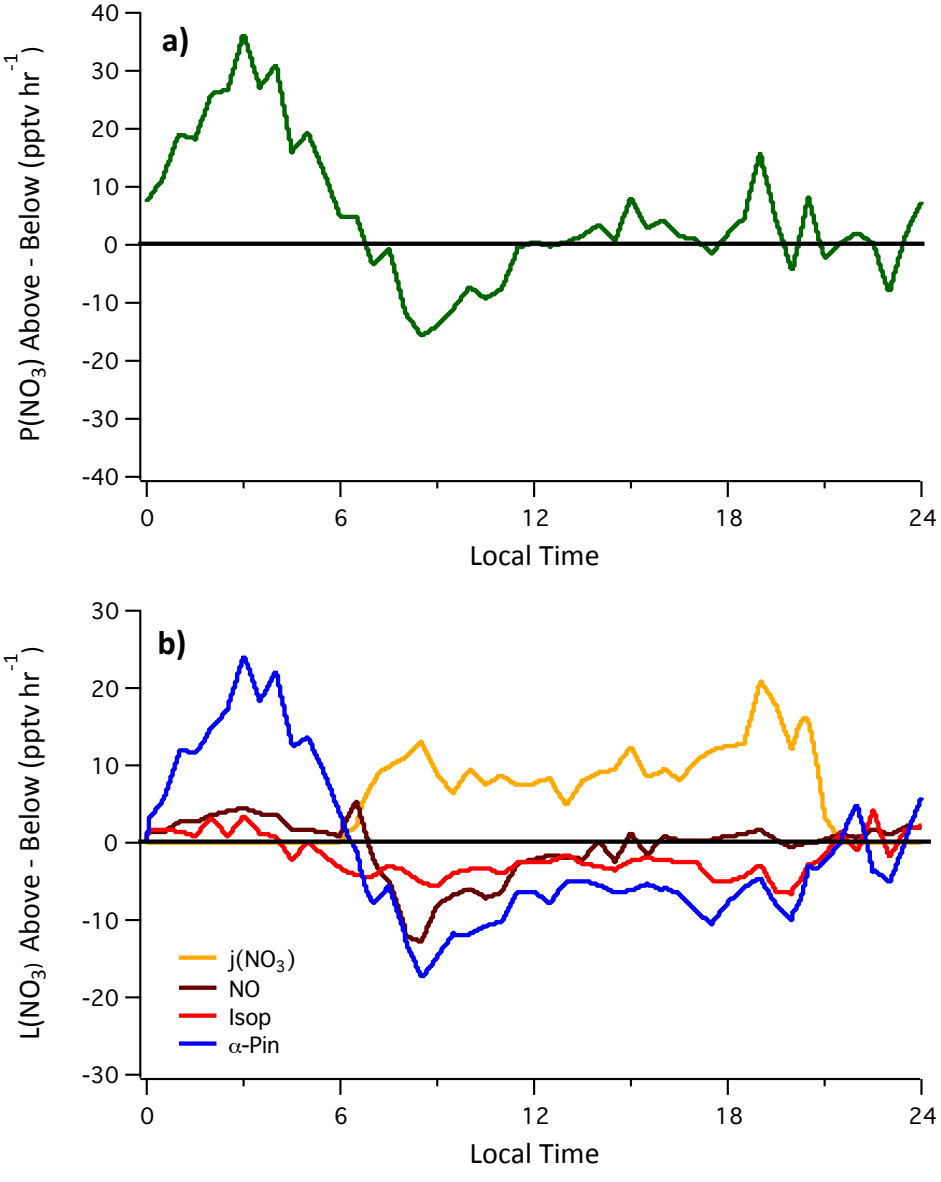

Figure 3. (**a**) Difference in NO_3 production rate above and below the forest canopy in the ambient CABINEX scenario. (**b**) Difference in individual NO_3 loss rates from photolysis, reaction with NO, oxidation of isoprene, and oxidation of α-pinene above and below the forest canopy in the ambient CABINEX scenario.

Atmos. Chem. Phys. Discuss., doi:10.5194/acp-2016-485, 2016
Manuscript under review for journal Atmos. Chem. Phys.
Published: 14 June 2016
© Author(s) 2016. CC-BY 3.0 License.

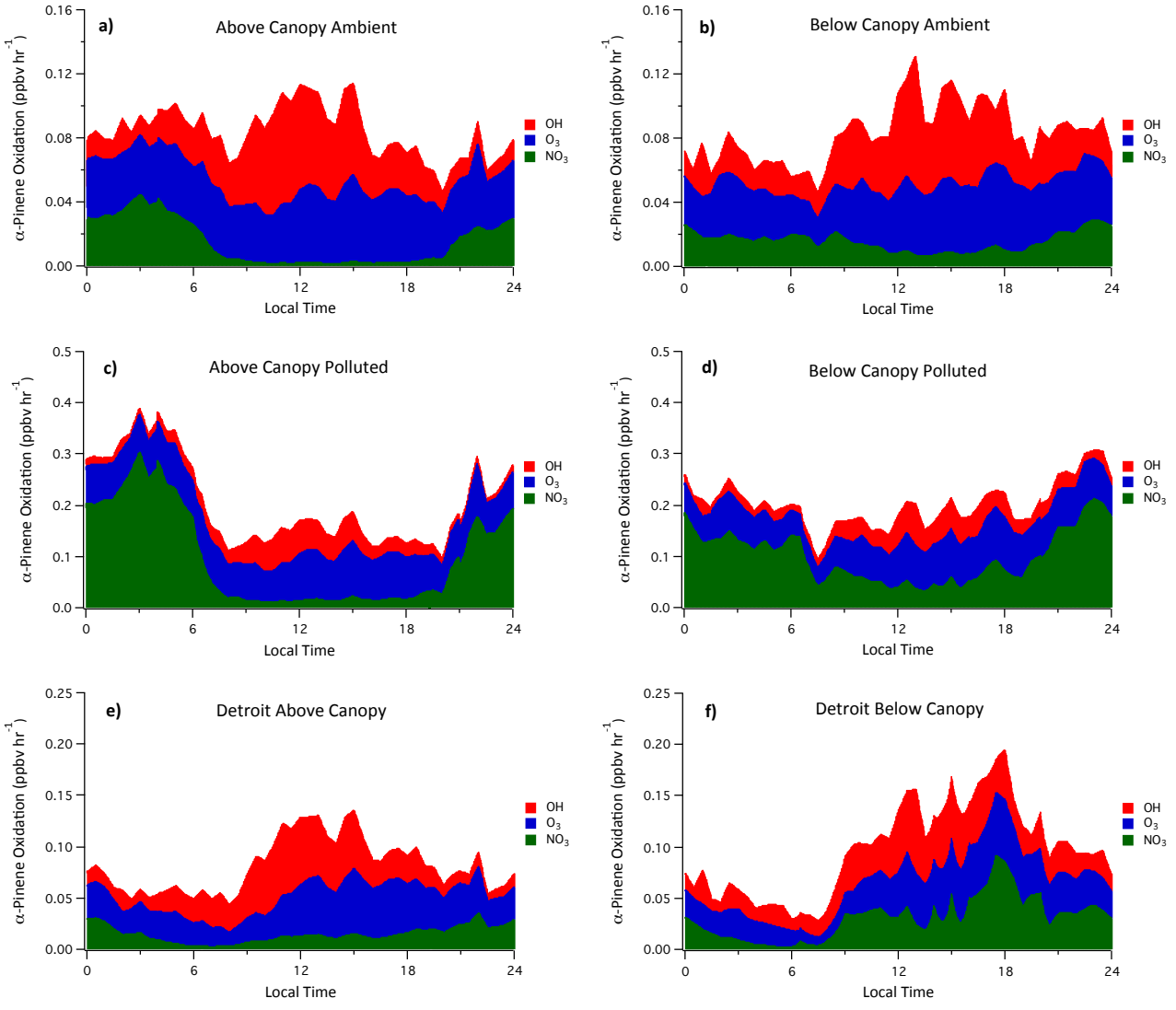

Figure 4. Modeled diurnal α-pinene oxidation rates by OH, O_3, and NO_3 for (**a**) ambient CABINEX above-canopy; (**b**) ambient CABINEX below-canopy; (**c**) artificially polluted above-canopy; (**d**) artificially polluted below-canopy; (**e**) Detroit above-canopy; (**f**) Detroit below-canopy.

Atmos. Chem. Phys. Discuss., doi:10.5194/acp-2016-485, 2016
Manuscript under review for journal Atmos. Chem. Phys.
Published: 14 June 2016
© Author(s) 2016. CC-BY 3.0 License.

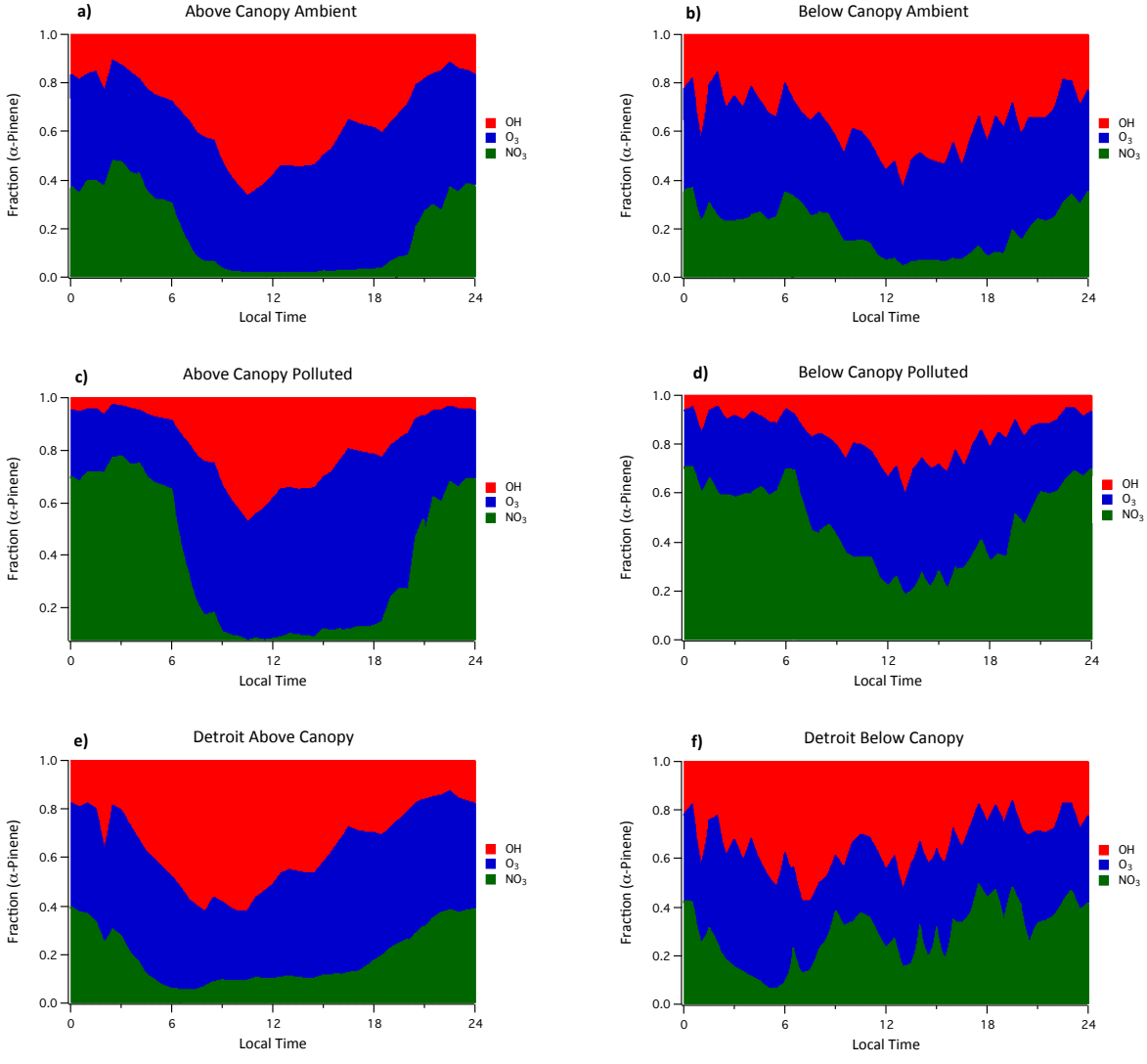

Figure 5. Modeled fractional α-pinene oxidation rates by OH, O_3, and NO_3 for (**a**) ambient CABINEX above-canopy; (**b**) ambient CABINEX below-canopy; (**c**) artificially polluted above-canopy; (**d**) artificially polluted below-canopy; (**e**) Detroit above-canopy; (**f**) Detroit below-canopy.

Atmos. Chem. Phys. Discuss., doi:10.5194/acp-2016-485, 2016
Manuscript under review for journal Atmos. Chem. Phys.
Published: 14 June 2016
© Author(s) 2016. CC-BY 3.0 License.

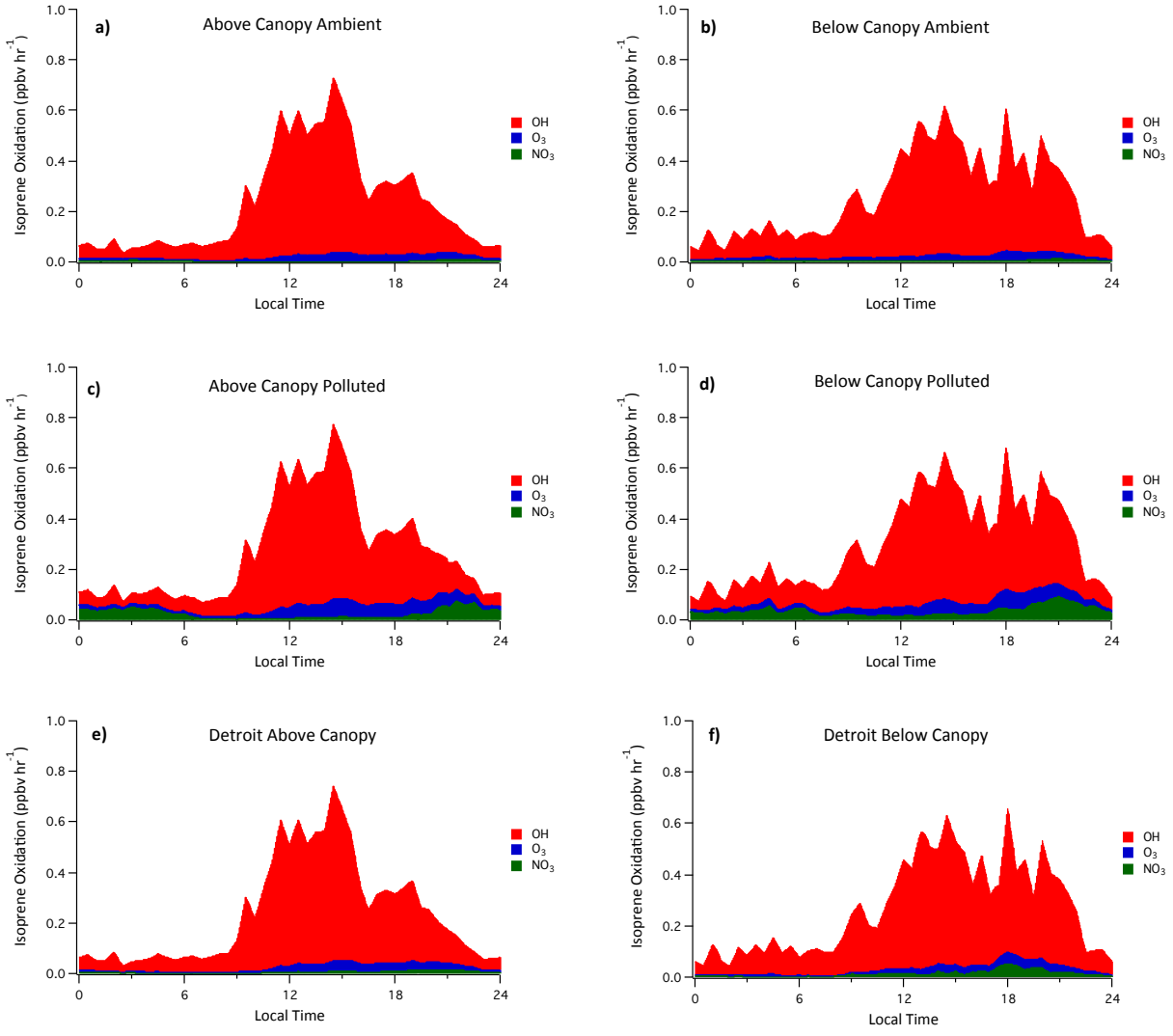

Figure 6. Modeled diurnal isoprene oxidation rates by OH, O_3, and NO_3 for (**a**) ambient CABINEX above-canopy; (**b**) ambient CABINEX below-canopy; (**c**) artificially polluted above-canopy; (**d**) artificially polluted below-canopy; (**e**) Detroit above-canopy; (**f**) Detroit below-canopy.

Atmos. Chem. Phys. Discuss., doi:10.5194/acp-2016-485, 2016
Manuscript under review for journal Atmos. Chem. Phys.
Published: 14 June 2016
© Author(s) 2016. CC-BY 3.0 License.

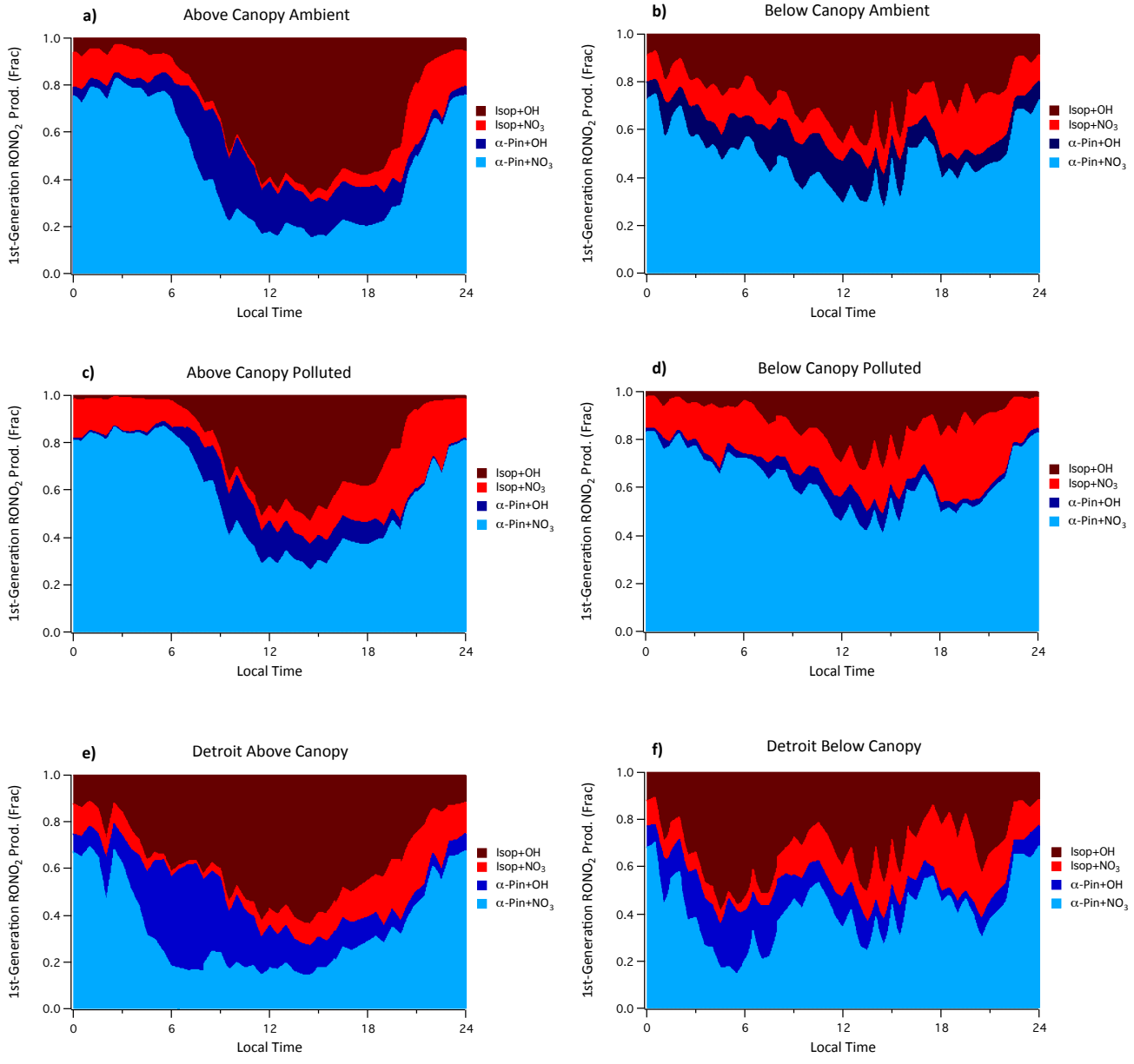

Figure 7. Modeled fractional first-generation organic nitrate ($RONO_2$) production by isoprene + OH, isoprene + NO_3, α-pinene + OH, and α-pinene + NO_3 for (**a**) ambient CABINEX above-canopy; (**b**) ambient CABINEX below-canopy; (**c**) artificially polluted above-canopy; (**d**) artificially polluted below-canopy; (**e**) Detroit above-canopy; (**f**) Detroit below-canopy.

Atmos. Chem. Phys. Discuss., doi:10.5194/acp-2016-485, 2016
Manuscript under review for journal Atmos. Chem. Phys.
Published: 14 June 2016
© Author(s) 2016. CC-BY 3.0 License.

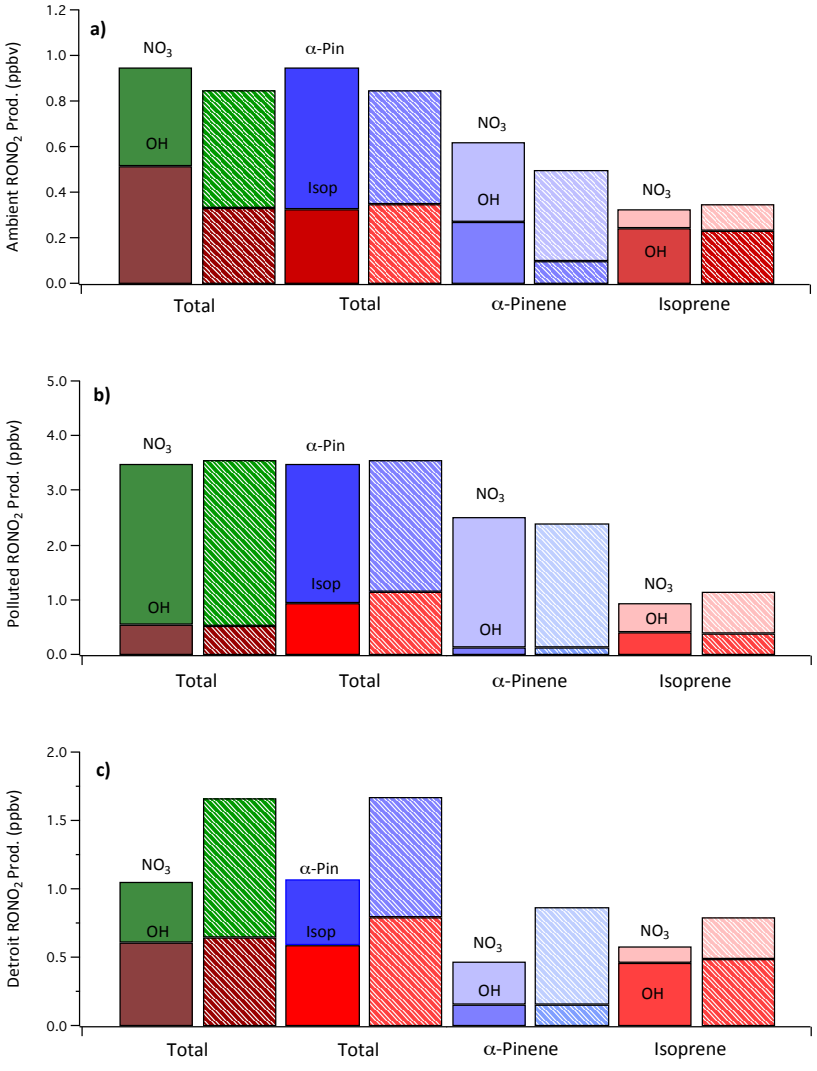

Figure 8. Daily production of 1st-generation organic nitrates ($RONO_2$) in (**a**) the ambient CABINEX scenario, (**b**) the artificially polluted scenario, and (**c**) the Detroit scenario. Solid bars indicate above-canopy results; hatched bars indicate below-canopy results. Columns 1 and 2 depict total daily $RONO_2$ production (above- and below-canopy respectively) (i.e. difference in cumulative mixing ratio of all 1st-generation $RONO_2$ between beginning and end of modeled diurnal period assuming no $RONO_2$ loss) with the relative contributions of NO_3 (green) and OH (brown) oxidation of the modeled BVOCs shown. Columns 3 and 4 depict total $RONO_2$ production divided into the relative contributions from α-pinene and isoprene oxidation. Columns 5 and 6 describe $RONO_2$ production solely from α-pinene oxidation divided into the relative contributions from NO_3 and OH oxidation, while columns 7 and 8 depict the same information as 5 and 6 but with respect to isoprene.

Atmos. Chem. Phys. Discuss., doi:10.5194/acp-2016-485, 2016
Manuscript under review for journal Atmos. Chem. Phys.
Published: 14 June 2016
© Author(s) 2016. CC-BY 3.0 License.

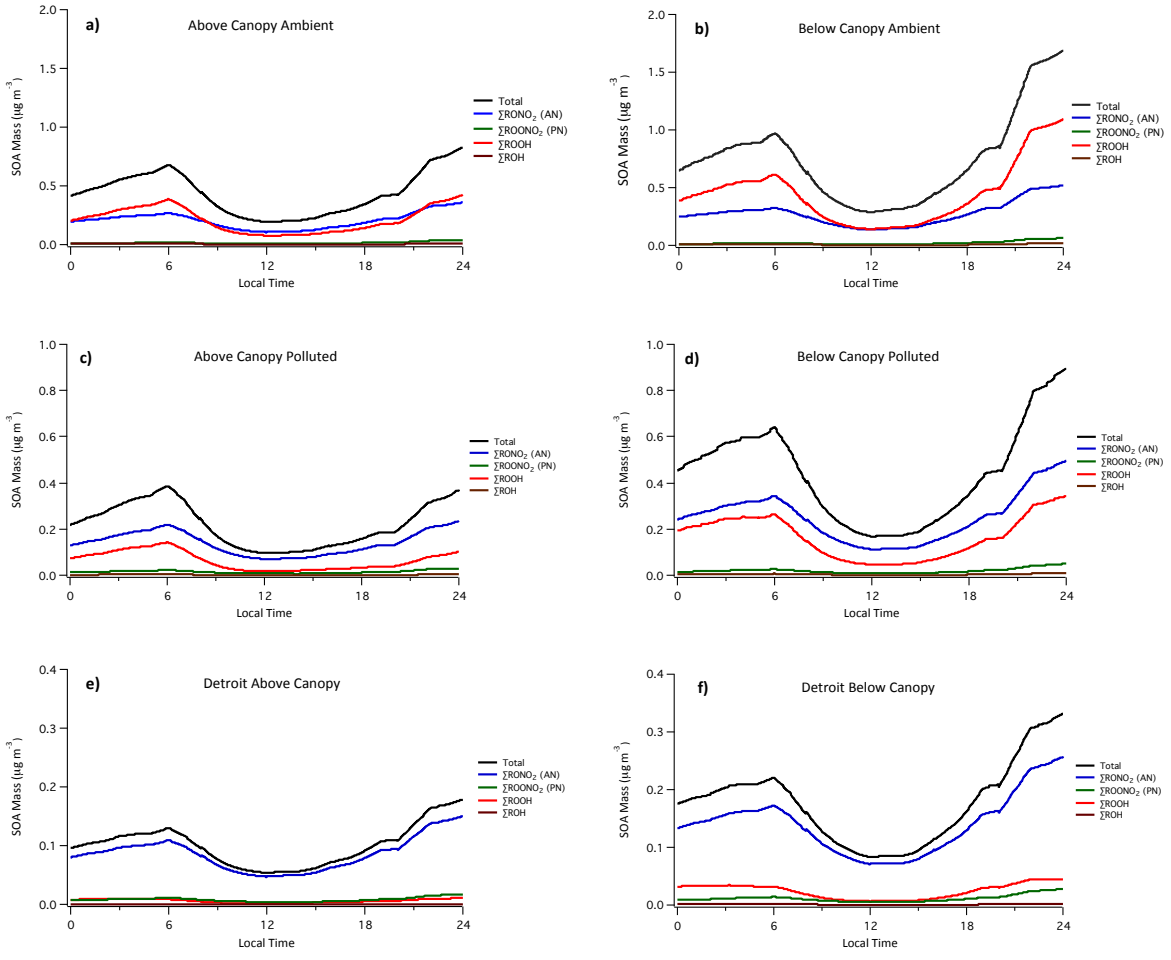

Figure 9. Modeled SOA diurnal profiles for (**a**) ambient CABINEX above-canopy; (**b**) ambient CABINEX below-canopy; (**c**) artificially polluted above-canopy; (**d**) artificially polluted below-canopy; (**e**) Detroit above-canopy; (**f**) Detroit below-canopy.

Atmos. Chem. Phys. Discuss., doi:10.5194/acp-2016-485, 2016
Manuscript under review for journal Atmos. Chem. Phys.
Published: 14 June 2016
© Author(s) 2016. CC-BY 3.0 License.

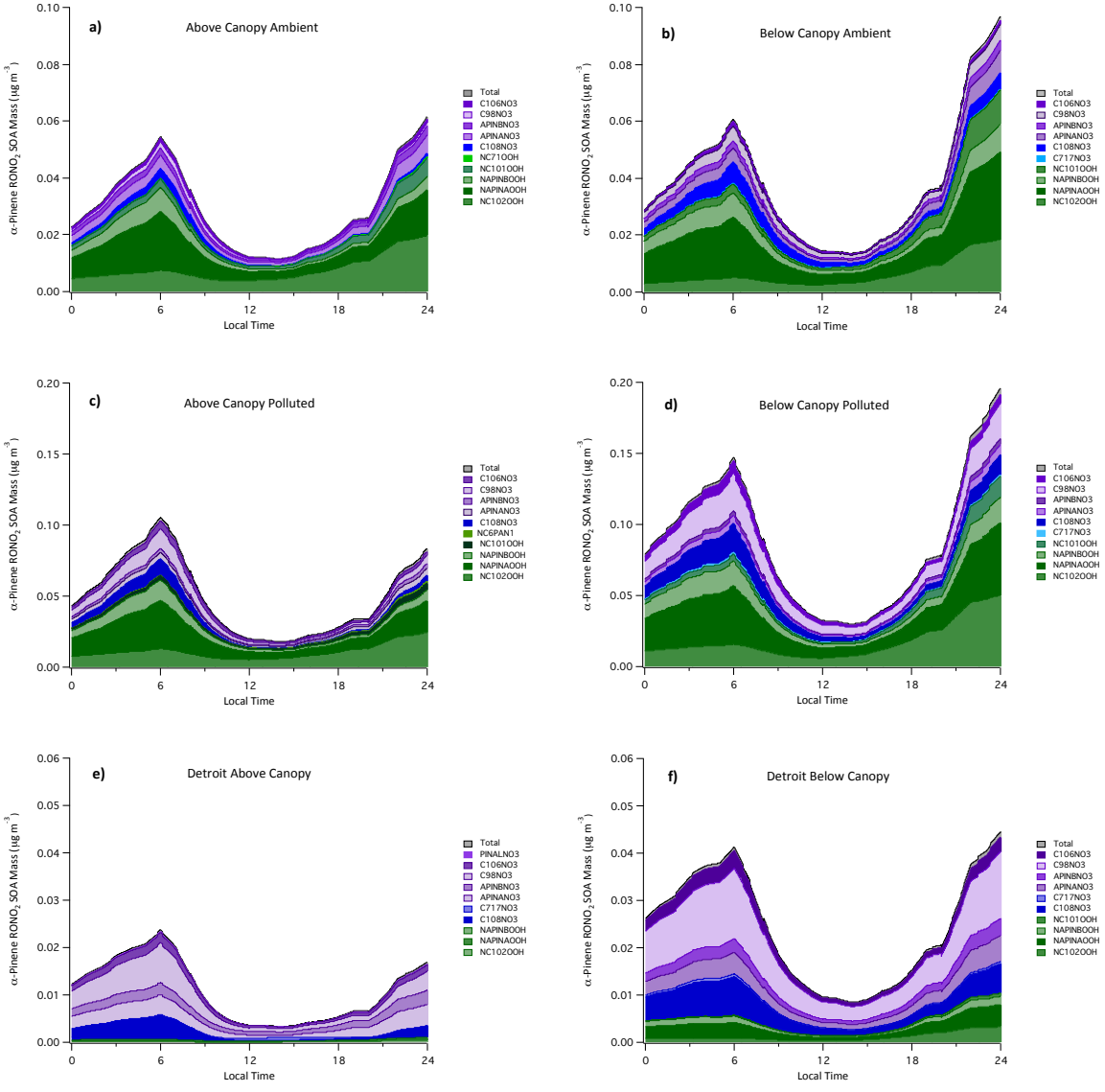

Figure 10. Diurnal profile of ten dominant α-pinene oxidation products formed from NO_3 oxidation (green), O_3 oxidation (blue), OH oxidation (red), and a mix of oxidants (purple) in $RONO_2$ SOA for (**a**) ambient CABINEX above-canopy; (**b**) ambient CABINEX below-canopy; (**c**) artificially polluted above-canopy; (**d**) artificially polluted below-canopy; (**e**) Detroit above-canopy; (**f**) Detroit below-canopy.

Atmos. Chem. Phys. Discuss., doi:10.5194/acp-2016-485, 2016
Manuscript under review for journal Atmos. Chem. Phys.
Published: 14 June 2016
© Author(s) 2016. CC-BY 3.0 License.

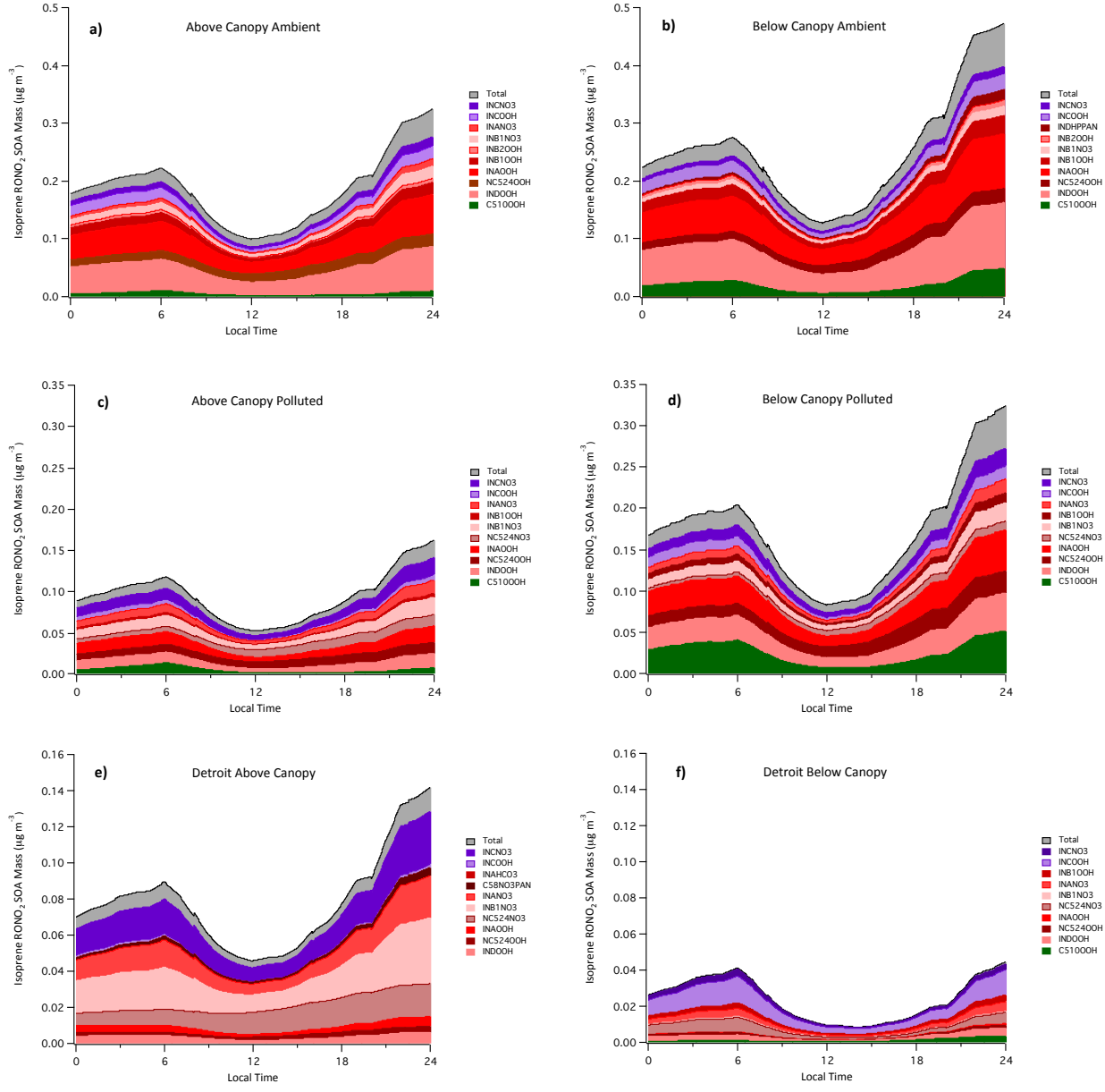

Figure 11. Diurnal profile of ten dominant isoprene oxidation products formed from NO_3 oxidation (green), O_3 oxidation (blue), OH oxidation (red), and a mix of oxidants (purple) in $RONO_2$ SOA for (**a**) ambient CABINEX above-canopy; (**b**) ambient CABINEX below-canopy; (**c**) artificially polluted above-canopy; (**d**) artificially polluted below-canopy; (**e**) Detroit above-canopy; (**f**) Detroit below-canopy.